NSWC TR 80-229

⑫ LEVEL Ⅱ

HYDRODYNAMIC COMPUTATIONS OF PRESSURES GENERATED BY STEAM PIPE RUPTURE

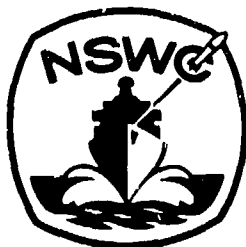BY   D. L. LEHTO   J. M. WARD

RESEARCH AND TECHNOLOGY DEPARTMENT

23 FEBRUARY 1981

NAVAL SURFACE WEAPONS CENTER

Dahlgren, Virginia 22448 ● Silver Spring, Maryland 20910

81 7 24 015

Final rept.
6 Mar - 30 Sep 78

REPORT DOCUMENTATION PAGE

| READ INSTRUCTIONS |
| BEFORE COMPLETING FORM |

1. REPORT NUMBER	2. GOVT ACCESSION NO.	3. RECIPIENT'S CATALOG NUMBER
NSWC/TR-80-229	AD-A102-046	

4. TITLE (and Subtitle)	5. TYPE OF REPORT & PERIOD COVERED
Hydrodynamic Computations of Pressures Generated by Steam Pipe Rupture	Final: 3/6/78-9/30/78
	6. PERFORMING ORG. REPORT NUMBER

7. AUTHOR(s)	8. CONTRACT OR GRANT NUMBER(s)
D. L. Lehto	Interagency Agreement No.
J. M. Ward	NRC-03-78-148

9. PERFORMING ORGANIZATION NAME AND ADDRESS	10. PROGRAM ELEMENT, PROJECT, TASK AREA & WORK UNIT NUMBERS
Naval Surface Weapons Center, White Oak Laboratory White Oak, Silver Spring, MD 20910	NRC,0,0, R15KB

11. CONTROLLING OFFICE NAME AND ADDRESS	12. REPORT DATE
	23 February 1981
	13. NUMBER OF PAGES
	53

14. MONITORING AGENCY NAME & ADDRESS(if different from Controlling Office)	15. SECURITY CLASS. (of this report)
	UNCLASSIFIED
	15a. DECLASSIFICATION/DOWNGRADING SCHEDULE

16. DISTRIBUTION STATEMENT (of this Report)

Approved for public release; Unlimited distribution

17. DISTRIBUTION STATEMENT (of the abstract entered in Block 20, if different from Report)

19. KEY WORDS (Continue on reverse side if necessary and identify by block number)

steam jet
two-dimensional hydrocode
two-phase flow

jet thrust
discharge coefficient

20. ABSTRACT (Continue on reverse side if necessary and identify by block number)

Calculations were made to determine the pressure loads generated by the impact of steam jets from a broken process pipe upon the inner wall of a surrounding concentric guard pipe. Longitudinal and circumferential breaks were considered, with various guard pipe diameters. The data obtained can be used in designing guard pipes for high-pressure steam process pipes. Circumferential and longitudinal 12.7 mm (0.5 in) and 50.8 mm (2.0 in) wide breaks in a 0.914 m (36 in). O. D. process pipe carrying 8.3 MPa (1200 psia)

DD FORM 1473 EDITION OF 1 NOV 65 IS OBSOLETE
1 JAN 73
S/N 0102-LF-014-6601

411563

20.   ABSTRACT (CONT.) >saturated steam were considered. Spaces between the process pipe and the guard pipe ranged from 12.7 mm (0.5 in) to 152.4 mm (6 in). The entire flow fields, including shock waves, were calculated with a two-dimensional hydrocode. The main loading on the guard pipe was determined to be the steady-flow pressure generated subsequent to the process pipe rupture. This pressure drops rapidly as the pipe spacing is increased, so from the standpoint of steam jets, pipe spacings of several inches are desirable.

FOREWORD

For the past twenty-four years, the Naval Surface Weapons Center has been involved in a research and consulting effort for both the Energy Research and Development Administration and the Nuclear Regulatory Commission concerned with the study of reactor vessel response to hypothetical core accidents and other types of dynamic loading events. As part of this effort, analyses of jet forces produced by ruptured steam process pipes on neighboring walls of reactor buildings have been performed. This report presents the computed results for impact loads from the ruptured process pipe on the inner wall of a surrounding concentric guard pipe for geometries consistent with reactor plant design guidelines.

This task was performed under Technical Assistance Contract "Guard Pipe, Process Pipe Interaction," FIN #B6467, Interagency Agreement No. NRC-03-78-148, monitored by J. J. Burns, Division of Systems Safety, NRR, Nuclear Regulatory Commission.

JAMES F. PROCTOR
By direction

Accession For	
NTIS GRA&I	✓
DTIC TAP	☐
Unannounced	☐
Justification	
By	
Distribution/	
Availability Codes	
Dist	Avail and/or Special
A	

1

CONTENTS

ILLUSTRATIONS

TABLES

SI UNITS

QUANTITY	SI UNIT NAME
FORCE	NEWTON (N)
MASS	KILOGRAM (kg)
TIME	SECOND (s)
LENGTH	METER (m)
FREQUENCY	HERTZ (Hz)
VOLUME	CUBIC METER (m^3)
SPEED	METER/SECOND (m/s)
DENSITY	KILOGRAM/CUBIC METER (kg/m^3)
ENERGY	JOULE (J)
WORK	NEWTON-METER (N-m)
PRESSURE	PASCAL (Pa)
IMPULSE	PASCAL-SECOND (Pa-s)
ENERGY FLUX DENSITY	METER-PASCAL (m-Pa)
TEMPERATURE	DEGREE KELVIN ($^\circ$K)

CONVERSION FACTORS

TO CONVERT	INTO	MULTIPLY BY
METERS	FEET	3.281
KILOGRAMS	POUNDS	2.2046
MEGAPASCALS (MPa)	psi	145.038
$m/kg^{1/3}$	$ft/lb^{1/3}$	2.5208
$kg^{1/3}/m$	$lb^{1/3}/ft$	0.3967
$kg^{1/3}$	$lb^{1/3}$	1.3015
$m/kg^{1/4}$	$ft/lb^{1/4}$	2.6929
kPa-s	psi-sec	0.14504
$kPa-s/kg^{1/3}$	$psi-sec/lb^{1/3}$	0.11144
m-kPa	in-psi	5.7073
$m-kPa/kg^{1/3}$	$in-psi/lb^{1/3}$	4.3852
$m^{4/3}/kg^{1/3}$	$ft^{4/3}/lb^{1/3}$	3.7453
$m^{5/6}/kg^{1/3}$	$ft^{5/6}/kg^{1/3}$	2.0678
kg/m^3	lb/ft^3	0.06243
FEET	METERS	0.3048
POUNDS	KILOGRAMS	0.4536
psi	MPa	0.0068946
$lb^{1/3}$	$kg^{1/3}$	0.7683
$ft/lb^{1/3}$	$m/kg^{1/3}$	0.3967
$lb^{1/3}/ft$	$kg^{1/3}/m$	2.5208
$ft/lb^{1/4}$	$m/kg^{1/4}$	0.3714
psi-sec	kPa-s	6.8947
$psi-sec/lb^{1/3}$	$kPa-s/kg^{1/3}$	8.9738
in-psi	m-kPa	0.17521
$in-psi/lb^{1/3}$	$m-kPa/kg^{1/3}$	0.22804
$ft^{4/3}/lb^{1/3}$	$m^{4/3}/kg^{1/3}$	0.2670
$ft^{5/6}/lb^{1/3}$	$m^{5/6}/kg^{1/3}$	0.4836
lb/ft^3	kg/m^3	16.017

CHAPTER 1

INTRODUCTION

1.1 BACKGROUND

Since 1956 the Naval Surface Weapons Center has been involved in a research and consulting effort for both the Energy Research and Development Administration and the Nuclear Regulatory Commission (NRC) concerned with the study of reactor vessel response to hypothetical core accidents and other types of dynamic loading events. In an earlier effort, NSWC provided to NRC preliminary calculations of pressure loads produced on neighboring walls by steam pipe ruptures. The task reported herein is a continuation of these calculations for the purpose of determining the pressure loads very close-in to the site of steam pipe rupture. Specifically, a series of hydrocode calculations were done to determine the fluid flow/pressure fields in regions bounded by an inner steam pipe and an outer guard pipe following simulated ruptures of the high-pressure inner steam pipe.

1.2 PROBLEM STATEMENT

A process pipe, filled with saturated steam at 8.3 MPa (1200 psia), was assumed to rupture instantaneously in either the circumferential or longitudinal direction (See Figure 1). The steam flowed out from the rupture, driving ambient air ahead of it, and impacted the inside surface of a guard pipe which surrounded the process pipe. The desired result was the pressure distribution along the guard pipe.

The analysis was performed in two phases. In the first phase, the proper equation of state for high-pressure saturated steam was evaluated, the appropriate finite difference grid scale for the problem geometry and flow conditions was determined, and a particular hydrocode for performing the calculations was selected. The second phase of the task determined the time-dependent internal pressure distribution on the guard pipe as a function of (a) direction of the pipe rupture (circumferential or longitudinal), (b) width of the pipe rupture, and (c) separation distance or gap between the process and guard pipes. The parameters for the seventeen process/guard pipe configurations that were computed are listed in Table 1.
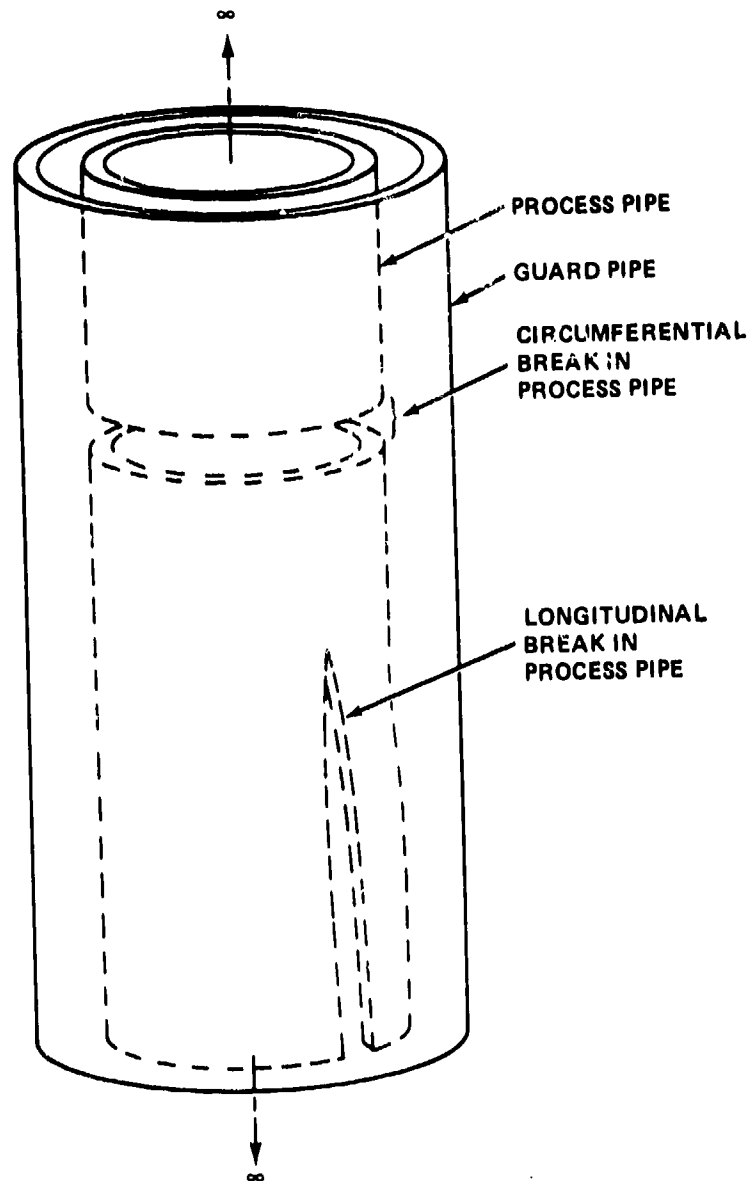
FIGURE 1. GEOMETRY OF BREAKS

TABLE 1
RUN PARAMETERS

METRIC UNITS--

RUN NO.	TUULI CALC NO.	SEE FIG.	PO (MPA)	PROC. PIPE THICK. (MM)	PROC. PIPE O.D. (M)	GUARD PIPE I.D. (M)	SPACE BETW. PIPES (MM)	BREAK WIDTH* (MM)
1	7879	13	8.274	50.8	0.914	1.016	50.8	12.7 L
2	7876	13	8.274	50.8	0.914	1.016	50.8	12.7 C
3	7873	12	8.274	50.8	0.914	1.016	50.8	50.8 L
4	7870	11	8.274	50.8	0.914	1.016	50.8	50.8 C
5	7880	13	8.274	50.8	0.914	1.118	101.6	12.7 L
6	7877	13	8.274	50.8	0.914	1.118	101.6	12.7 C
7	7874	12	8.274	50.8	0.914	1.118	101.6	50.8 L
8	7871	11	8.274	50.8	0.914	1.118	101.6	50.8 C
9	7881	13	8.274	50.8	0.914	1.219	152.4	12.7 L
10	7878	13	8.274	50.8	0.914	1.219	152.4	12.7 C
11	7875	12	8.274	50.8	0.914	1.219	152.4	50.8 L
12	7872	11	8.274	50.8	0.914	1.219	152.4	50.8 C
13	7882	14	6.895	37.3	0.813	1.086	136.7	50.8 L
14	7883	14	6.895	37.3	0.813	1.086	136.7	50.8 C
15	7884	14	6.610	37.3	0.813	1.086	136.7	50.8 C
16	7889	12	8.274	50.8	0.914	0.940	12.7	50.8 L
17	7888	12	8.274	50.8	0.914	0.965	25.4	50.8 L

ENGLISH UNITS--

RUN NO.	TUULI CALC NO.	SEE FIG.	PO (PSIA)	PROC. PIPE THICK. (IN)	PROC. PIPE O.D. (IN)	GUARD PIPE I.D. (IN)	SPACE BETW. PIPES (IN)	BREAK WIDTH* (IN)
1	7879	13	1200	2.0	36.	40.	2.0	0.5 L
2	7876	13	1200	2.0	36.	40.	2.0	0.5 C
3	7873	12	1200	2.0	36.	40.	2.0	2.0 L
4	7870	11	1200	2.0	36.	40.	2.0	2.0 C
5	7880	13	1200	2.0	36.	44.	4.0	0.5 L
6	7877	13	1200	2.0	36.	44.	4.0	0.5 C
7	7874	12	1200	2.0	36.	44.	4.0	2.0 L
8	7871	11	1200	2.0	36.	44.	4.0	2.0 C
9	7881	13	1200	2.0	36.	48.	6.0	0.5 L
10	7878	13	1200	2.0	36.	48.	6.0	0.5 C
11	7875	12	1200	2.0	36.	48.	6.0	2.0 L
12	7872	11	1200	2.0	36.	48.	6.0	2.0 C
13	7882	14	1000	1.47	32.	42.75	5.38	2.0 L
14	7883	14	1000	1.47	32.	42.75	5.38	2.0 C
15	7884	14	1250	1.47	32.	42.75	5.38	2.0 C
16	7889	12	1200	2.0	36.	37.	0.5	2.0 L
17	7888	12	1200	2.0	36.	38.	1.0	2.0 L

*C=CIRCUMFERENTIAL
L=LONGITUDINAL

CHAPTER 2

ANALYTICAL SOLUTIONS

For a free compressible jet expanding to ambient pressure, the total jet thrust for an ideal gas as given by Reference 1 (slightly modified) is

$$T/A_e = C_1 P_0 - P_\infty$$

where T = Jet thrust = Total force on a large normally-impacted plate

A_e = Effective area of process pipe break

P_0 = Pipe reservoir pressure

P_∞ = Ambient pressure

$C_1 = (1 + \gamma)(2/(\gamma + 1))^{\gamma/(\gamma-1)}$

γ = Specific heat ratio

The coefficient C_1 is a weak function of γ, being 1.255 for γ = 1.3 and 1.229 for γ = 1.1058.

This solution, or any other such simple solution, is not adequate here because

(1) The gap between the pipes is relatively narrow in comparison with the pipe dimensions, and backpressure on the outside of the process pipe must be accounted for in a force balance;

(2) The non-uniform filling of the gap between the process and guard pipes with steam and compressed air makes P_∞ ill-defined;

(3) The nozzle discharge coefficient is not known a priori to obtain the effective value of A_e for the break in the process pipe;

(4) Time-dependent pressures must be considered here initially to obtain the early-on transient airshock/steam shock contributions to the guard pipe loading;

---

[1]Moody, F. J., "Prediction of Blowdown Thrust and Jet Forces," ASME Paper 69-HT-31, ASME-AIChE Heat Transfer Conference, Minneapolis, Minn., Aug 1969.

(5) The distribution of pressure along the guard pipe inside surface, not just the total force, is needed for future structural response calculations.

The total force calculations are useful, however, for comparing with integrated results obtained from the hydrocode computations. These comparisons are discussed later.

CHAPTER 3

HYDROCODE SOLUTIONS

This was a problem well suited for an Eulerian (rather than Lagrangean) hydrocode since there is much distortion in the flow. In the initial phase of the analysis two hydrocodes were used, TUULI and CSQ.

TUULI* is a two-dimensional Eulerian hydrocode, written in 1975 at NSWC by D. Lehto. Full documentation is not yet available. The code is based on the fluid-in-cell (FLIC) method (REFERENCE 2) where the calculation is done in four steps per time cycle:

1) The accelerations are calculated from the pressure gradients and new provisional velocities are calculated (without convection).

2) The provisional velocities are used to calculate the pdV work done on each zone; this gives provisional internal energies (still without convection).

3) The material transport (convection) is done with the provisional velocities and energies.

4) Any adjustments ...eeded to conserve both energy and momentum are made. Any kinetic energy correction needed for momentum conservation is taken from (or added to) the internal energy. These adjustments are necessary because the flow mixes dissimilar flows from adjacent zones, and both kinetic energy and momentum cannot be conserved in a mixing process. This fourth step is explicitly done in TUULI because internal energy is transported; it is implicitly done in the original FLIC code because total energy is transported. This is a trivial arbitrary choice.

TUULI handles two materials (here, steam and air) and has an option for assigned inflow in any chosen zones (used extensively in these calculations). The grid is composed of fixed rectangular zones. Shocks are handled by the quadratic artificial viscosity method.

---

[2]Gentry, R. A., Martin, R. E., and Daly, B. J., "An Eulerian Differencing Method for Unsteady Compressible Flow Problems," J. Comput. Phys. 1, pp 87-118, 1966.

*Until now, this code was called TUTTI, However, this is also the name of a Los Alamos Scientific Laboratory equation-of-state program (J. Appl. Phys. 51 (10) 5368 (1980)). Thus, the name change: TUTTI to TUULI.

CSQ is a two-dimensional Eulerian hydrocode written at the Sandia Laboratories. Documentation for this code is provided in Reference 3. In this method, the calculation is performed in two main phases:

1) The finite difference analogs of the complete two-dimensional Lagrangean equations are solved during each time cycle.

2) At the end of the time cycle, the code rezones the mesh back to the original configuration.

The net result of the rezoning is an Eulerian calculation. The version of CSQ described in Reference 3 handles only two materials in any chosen zone. The grid is composed of fixed rectangular zones. Shocks are handled by the quadratic artificial viscosity method.

The computations were performed on a CYBER 176 at the Air Force Weapons Laboratory in Albuquerque, New Mexico over telephone lines from NSWC.

3.1 ZONE SIZE SELECTION

Both TUULI and CSQ face the same limitations on available computer size and cost of computer time. Care was taken to choose a calculation mesh just fine enough to give the desired accuracy; this was done by simply trying progressively finer meshes until the overpressure loading on the guard pipe inside wall no longer changed significantly. The final mesh selected was 0.315 zones/mm (8 zones/in) within the channel formed by the break after it was determined that reduction of the mesh size down to 0.630 zones/mm (16 zones/in) produced no significant effect on the calculated flow. The mesh was nonuniform and varied for each problem geometry, being fine in the channel and near the impact area on the guard pipe and progressively coarser with increasing distance from the region of interest.

3.2 ZONE SHAPE LIMITATION

Both hydrocodes are limited to rectangular zones. This makes the longitudinal-break problem awkward, because the concentric circles needed to represent the problem cross section would have to be made up of rectangular steps (See Figure 2). For the longitudinal-break calculations, the pipes were straightened out into parallel planes as shown in the figure; this is expected to be a good approximation since the separation distances between pipes are relatively small compared with the pipe radii for the geometries investigated here. No problem arose in setting up the mesh with rectangular zones for the circumferential-break calculations because all bounding surfaces could be represented by straight lines. The computing mesh for the flat-plate approximation for the longitudinal break shown in Figure 2 looks similar to the mesh for the circumferential break; however, the latter has axial symmetry.

---

[3]Thompson, S. L., "CSQ -- A Two Dimensional Hydrodynamic Program with Energy Flow and Material Strength," Sandia Labs. SAND 74-0122, Aug 1975.

13

GUARD PIPE

PROCESS PIPE

SLIT

TRUE GEOMETRY   REGION OF   PLANE OF
                 INTEREST   SYMMETRY

GUARD PIPE

PROCESS PIPE

SLIT

ORTHOGONAL GRID APPROXIMATION (NOT USED)

PROCESS PIPE

GUARD PIPE

SLIT

PLANE OF   REGION OF
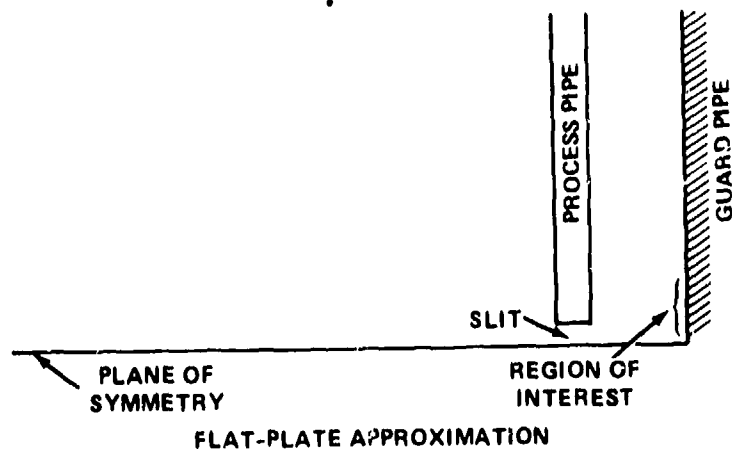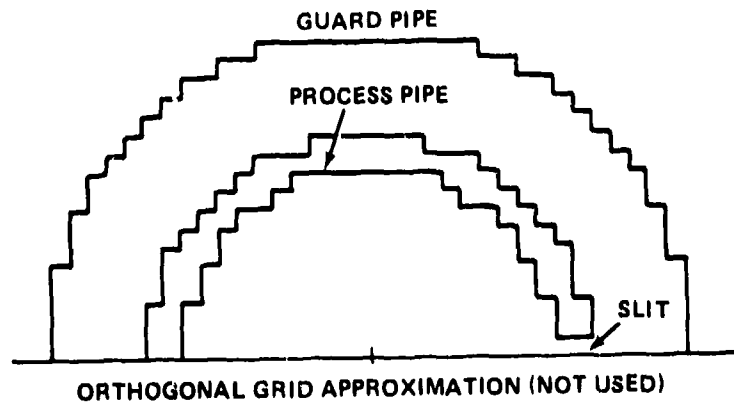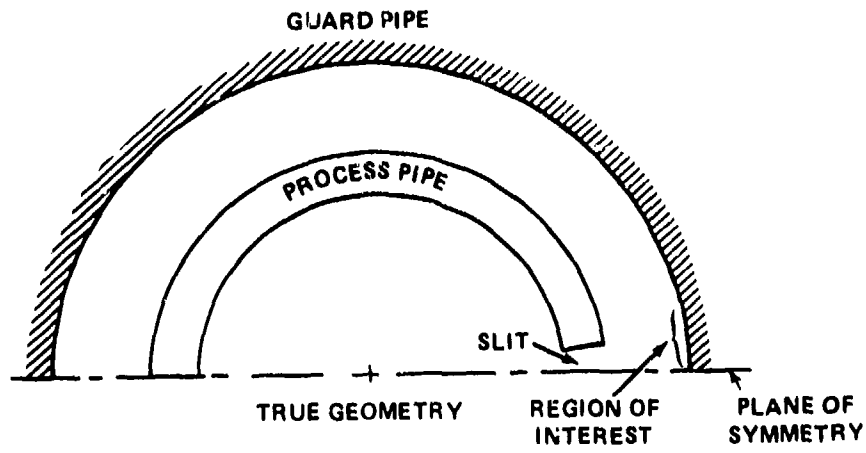SYMMETRY   INTEREST

FLAT-PLATE APPROXIMATION

FIGURE 2. GEOMETRY FOR LONGITUDINAL BREAK

3.3 EQUATIONS OF STATE

When the steam pressure drops as it leaves the ruptured process pipe, condensation takes place and the resulting two-phase flow expands isentropically. For example, the isentropic exponent for equilibrium flow (i.e., equilibrium between the vapor and droplet phases) is 1.1058 (Table 2) for saturated steam at 8.3 MPa (1200 psia).* However, it takes a finite time for the vapor to condense into droplets. If this relaxation were a relatively slow process with respect to the expansion, the expanding steam would continue to behave as a pure vapor. On the vapor side of the saturation line, the adiabatic exponent is 1.2592; a frozen flow would be expected to maintain this exponent beyond the saturation line. The actual flow would lie between these two states during the expansion process. Referring to Figure 3 (taken from Reference 5), the TI-curve is the equilibrium flow isentrope and the I'-curve segment below the saturated vapor curve (SV) is the frozen flow isentrope. The actual curve, nonequilibrium flow designated ACT, for the two-phase steam mixture which takes into account the kinetics of the relaxation/condensation process falls somewhere in between the TI and the I' curves as shown in the figure.

The effect of nonequilibrium flow (delay in condensation) was bounded by performing hydrocode calculations with adiabatic exponents (γ) for both the frozen and the equilibrium flow conditions. An ideal-gas equation of state,

$$P = (\gamma - 1)\rho E ,$$

was used to give the isentrope,

$$P\rho^{-\gamma} = \text{constant},$$

where P is pressure, ρ is density, and E is internal energy. The results, given in Figure 4 for a typical circumferential-break geometry, indicate that nonequilibrium flow corrections to the pressure loading on the guard pipe opposite the pipe break are negligible. Equilibrium flow was assumed for the rest of the hydrocode calculations.

---

*Steam table (Reference 4) pressure-volume data were fitted (on a log-log scale) with straight lines to get the adiabatic exponents given in Table 2.

[4]Keenan, J. H. and Keyes, F. G., Thermodynamic Properties of Steam, Including Data for the Liquid and Solid Phases, 1st ed., Wiley, New York, 1936.

[5]Zel'dovich, Ya. B., and Raizer, Yu, P., Physics of Shock Waves and High Temperature Hydrodynamic Phenomena, Volume II, ed. by W. D. Hayes and R. F. Probstein, Academic Press, New York, 1967.

TABLE 2
SATURATED STEAM DATA

METRIC UNITS--

PRESSURE	(MPA)	6.895	8.274	8.618
SPECIFIC VOLUME	(M3/MG)	27.82	22.59	21.54
DENSITY	(MG/M3)	0.03595	0.04426	0.04644
TEMPERATURE	(K)	557.98	570.51	573.39
ENTROPY	(J/KG.K)	5818.	5722.	5699.

ADIABATIC CONSTANT ON VAPOR SIDE		1.2623	1.2592	1.2777
ADIABATIC CONSTANT ON 2-PHASE SIDE		1.0866	1.1058	1.1046

ENGLISH UNITS--

PRESSURE	(PSIA)	1000	1200	1250
SPECIFIC VOLUME	(FT3/LB)	0.4456	0.3619	0.3450
TEMPERATURE	(F)	544.67	567.22	572.42
ENTROPY	(BTU/F.LB)	1.3897	1.3667	1.3612

TABLE 3
EXIT CONDITIONS AT SLIT

8.274 MPA (1200 PSIA) SATURATED STEAM. GAMMA=1.1058
BREAK WIDTH=50.8 MM (2 IN), PIPE THICKNESS=50.8 MM (2 IN).

DISTANCE FROM MIDPLANE OF BREAK (MM)	PRESSURE (MPA)	DENSITY (G/MM3)	PARTICLE VELOCITY (M/S)	SOUND SPEED (M/S)	MASS FLUX (G/M2/US)
1.6	2.613	15.52	609.8	431.5	9.464
4.8	2.616	15.52	608.5	431.7	9.444
7.9	2.618	15.52	605.9	431.9	9.404
11.1	2.617	15.52	601.1	431.8	9.329
14.3	2.606	15.52	591.7	430.9	9.183
17.5	2.573	15.52	573.2	428.2	8.896
20.6	2.506	15.52	535.6	422.5	8.316
23.8	2.403	15.52	463.7	413.8	7.197
SONIC		27.66	472.8	472.8	12.05

I — ISENTROPE FOR VAPOR
I' — ISENTROPE FOR SUPERSATURATED (SUPERCOOLED) VAPOR
SV — SATURATED VAPOR CURVE
O — SATURATED POINT
TI — ISENTROPE FOR EQUILIBRIUM
       TWO· PHASE VAPOR · LIQUID SYSTEM
ACT — ACTUAL CURVE FOR THE VAPOR · LIQUID DROP SYSTEM
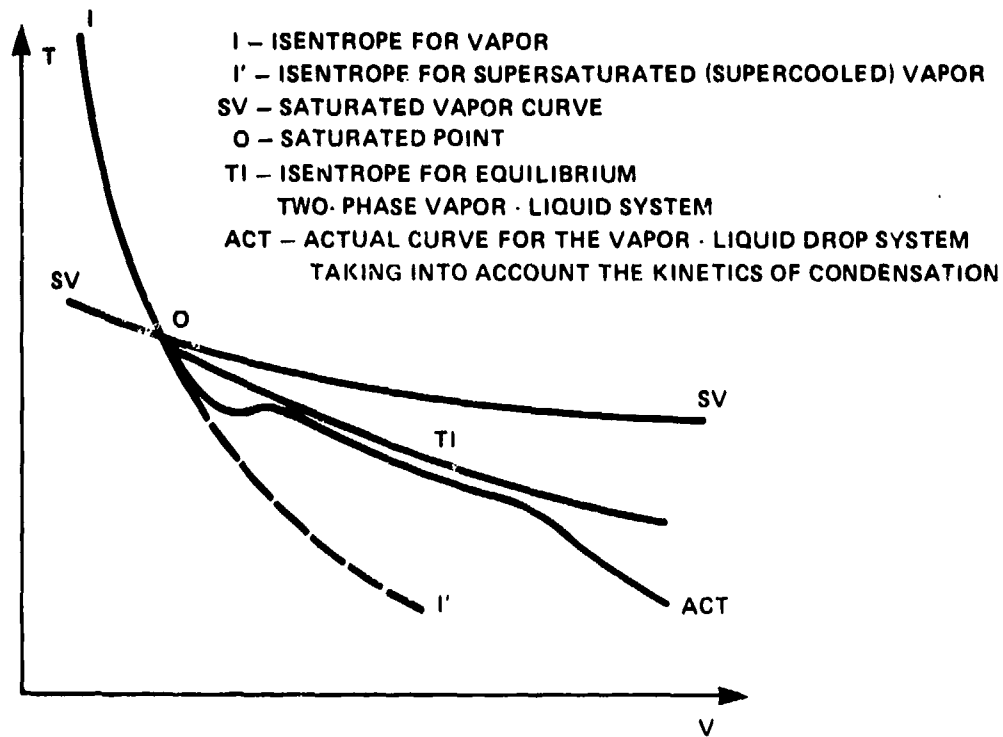   TAKING INTO ACCOUNT THE KINETICS OF CONDENSATION

FIGURE 3. T·V DIAGRAM FOR CONDENSATION IN AN ISENTROPIC VAPOR EXPANSION
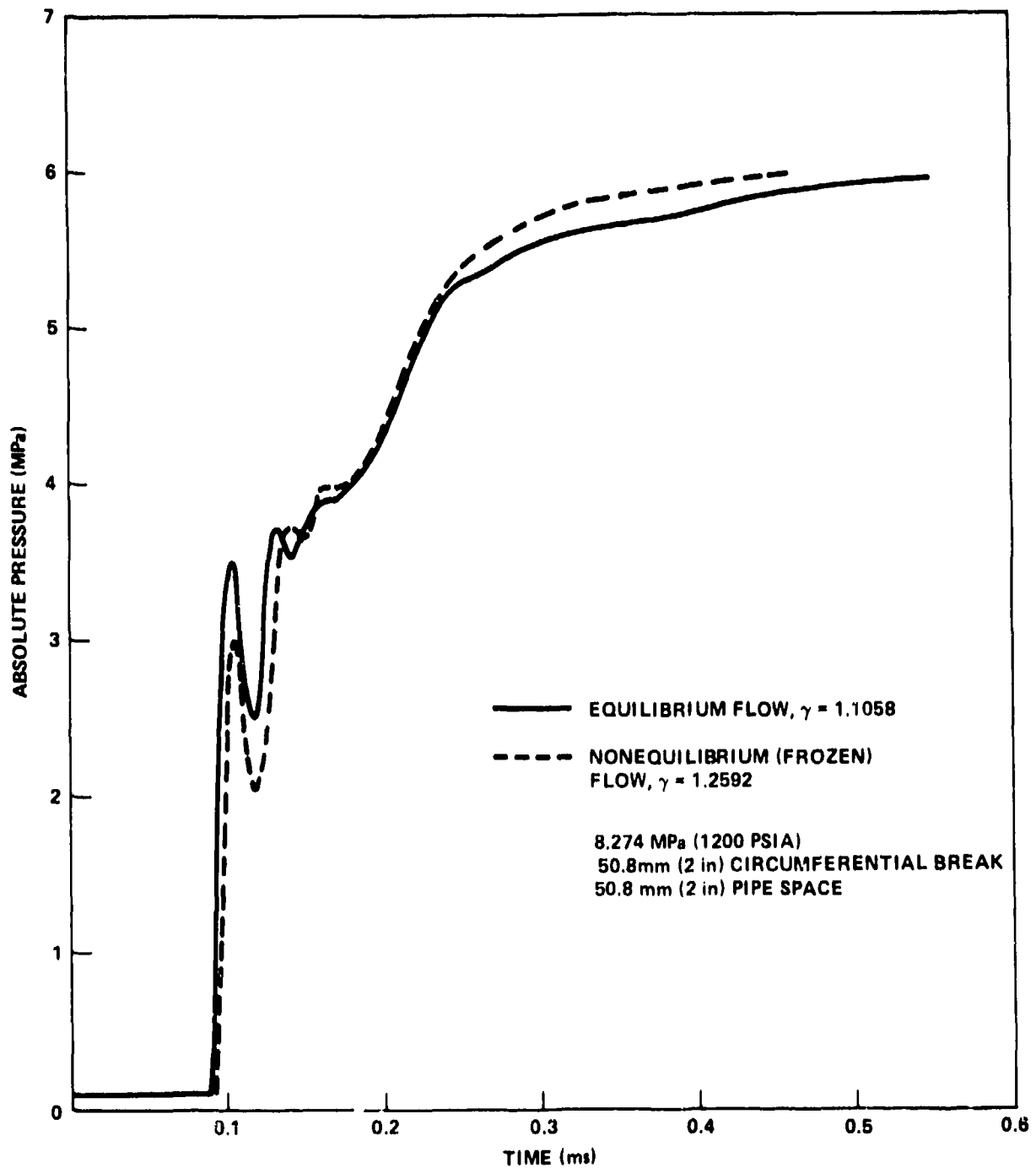
FIGURE 4. EFFECT OF THERMODYNAMIC NONEQUILIBRIUM ON PRESSURE ON GUARD PIPE OPPOSITE THE BREAK

The air in the gap between the process and guard pipes was treated as an ideal gas with γ = 1.4. The air in the gap was initially set to an average temperature of 422 K (300° F) for all the hydrocode calculations. This value was determined by performing a steady one-dimensional heat conduction analysis (see Reference 6, p. 37) for a steam pipe surrounded by an air gap, a guard pipe, and an ambient atmosphere with free convection.

3.4 HYDROCODE SELECTION

TUULI and CSQ give essentially the same results, as expected. This is demonstrated in Figure 5 which presents the pressure versus time history from each code at the guard pipe surface directly opposite the circumferential break for Run No. 4 listed in Table 1. The small oscillations are unresolved airshock reflections between the nose of the steam jet and the guard pipe wall. They are considered insignificant in terms of pipe response to the pressure loads.

TUULI was the hydrocode chosen for the remainder of the calculations because the authors are more familiar with it than with CSQ.

---

[6] Kreith, F., _Principles of Heat Transfer_, 2nd ed., International Textbook Co., Scranton, Pa., 1965.
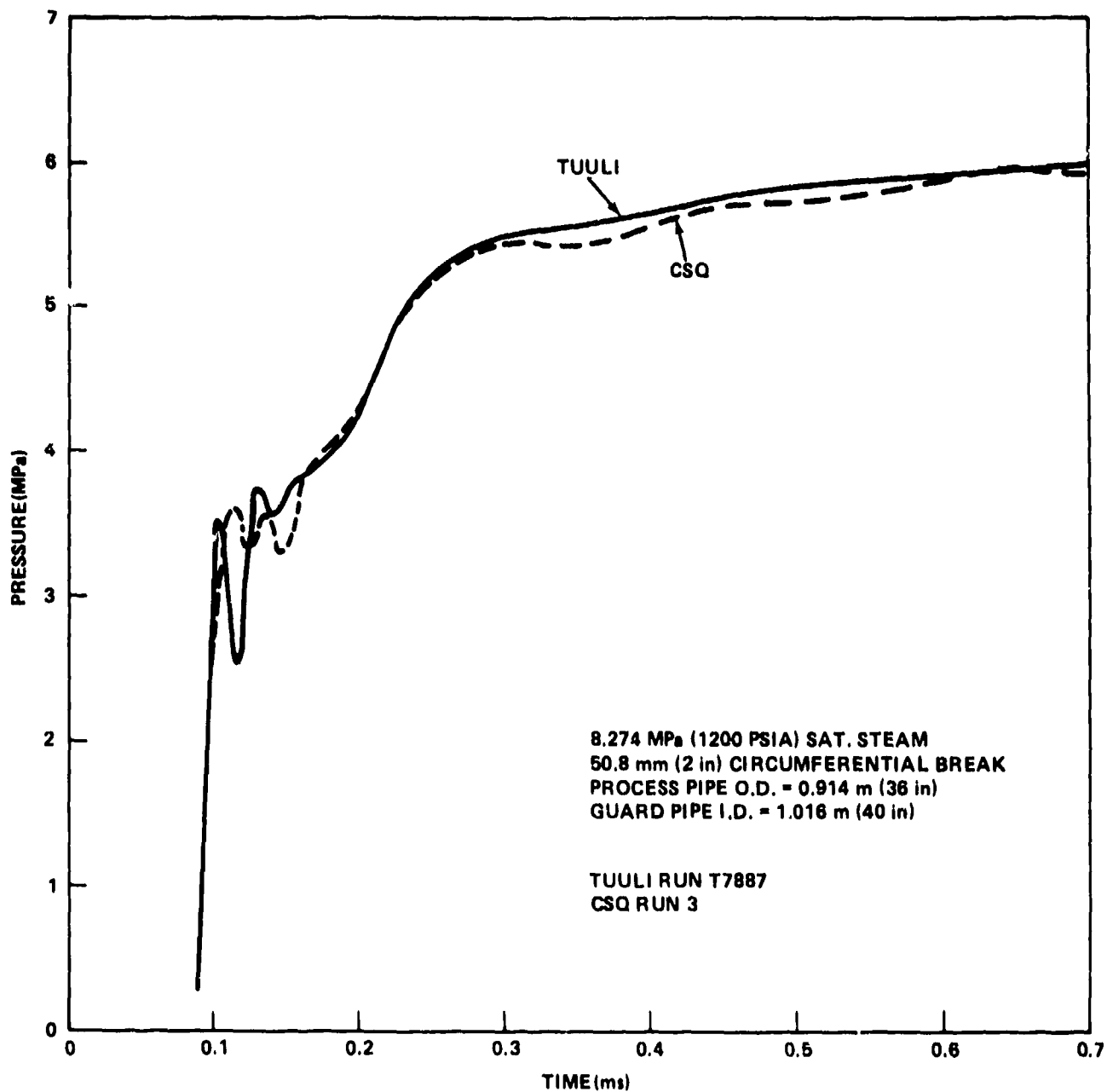
FIGURE 5. TUULI AND CSQ CODE PRESSURE VS TIME ON GUARD PIPE OPPOSITE THE BREAK

CHAPTER 4

HYDROCODE RESULTS

The expected flow phenomena following an instantaneous break in the process pipe (for the circumferential-break geometry) are shown in Figure 6. A rarefaction wave recedes into the process pipe steam reservoir. A steam plume jets from the break in the process pipe into the air gap between the process and guard pipes. Sonic conditions are attained within the break and the flow becomes choked. An airshock precedes the steam jet and a stationary shock front (in the steam) is formed which stands off at some distance from the guard pipe inner wall.

In section 4.1 several elements of the flow phenomena -- rarefaction wave, sonic flow in the process pipe break, and discharge coefficient for the break -- are discussed. These elements allow a substantial simplification of the flow field calculations. The flow internal to the process pipe need only be computed once (with a hydrocode) for each initial steam flow condition. Following this, truncated flow field computations are then performed for the different process/ guard pipe geometries. The truncated flow field calculation involves specifying the steady outflow from the process pipe exit and then computing the flow field for the intervening space between the process pipe and the guard pipe.

Section 4.2 discusses the following aspects of the flow field for the region between the process pipe and the guard pipe:

1) The pressure loads on the guard pipe wall produced by the airshock preceding the steam plume;

2) The transient initial pressure loads produced by the steam plume on the guard pipe wall;

3) The stationary shock in the vicinity of the guard pipe wall; and

4) The maximum pressure loads on the guard pipe wall that are established by the steady flow of the steam exiting from the process pipe break.

4.1 OUTFLOW FROM PROCESS PIPE

RAREFACTION WAVE. A rarefaction wave runs from the break into the steam in the process pipe. For a circumferential break, this wave reflects from the pipe axis and part of it comes back into the break. Figure 7 shows the guard pipe wall reflected pressure versus time for such a calculation carried out far enough in time to follow the propagation of the reflected rarefaction wave to
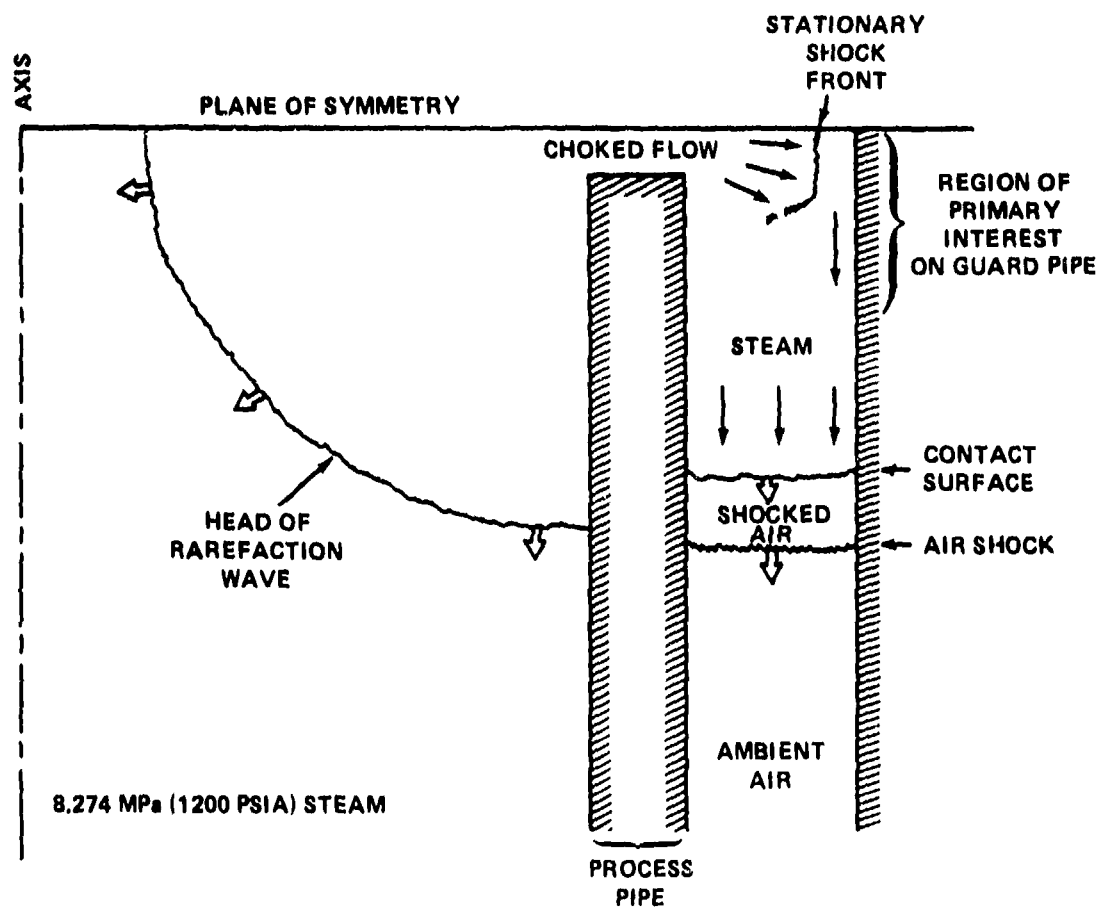
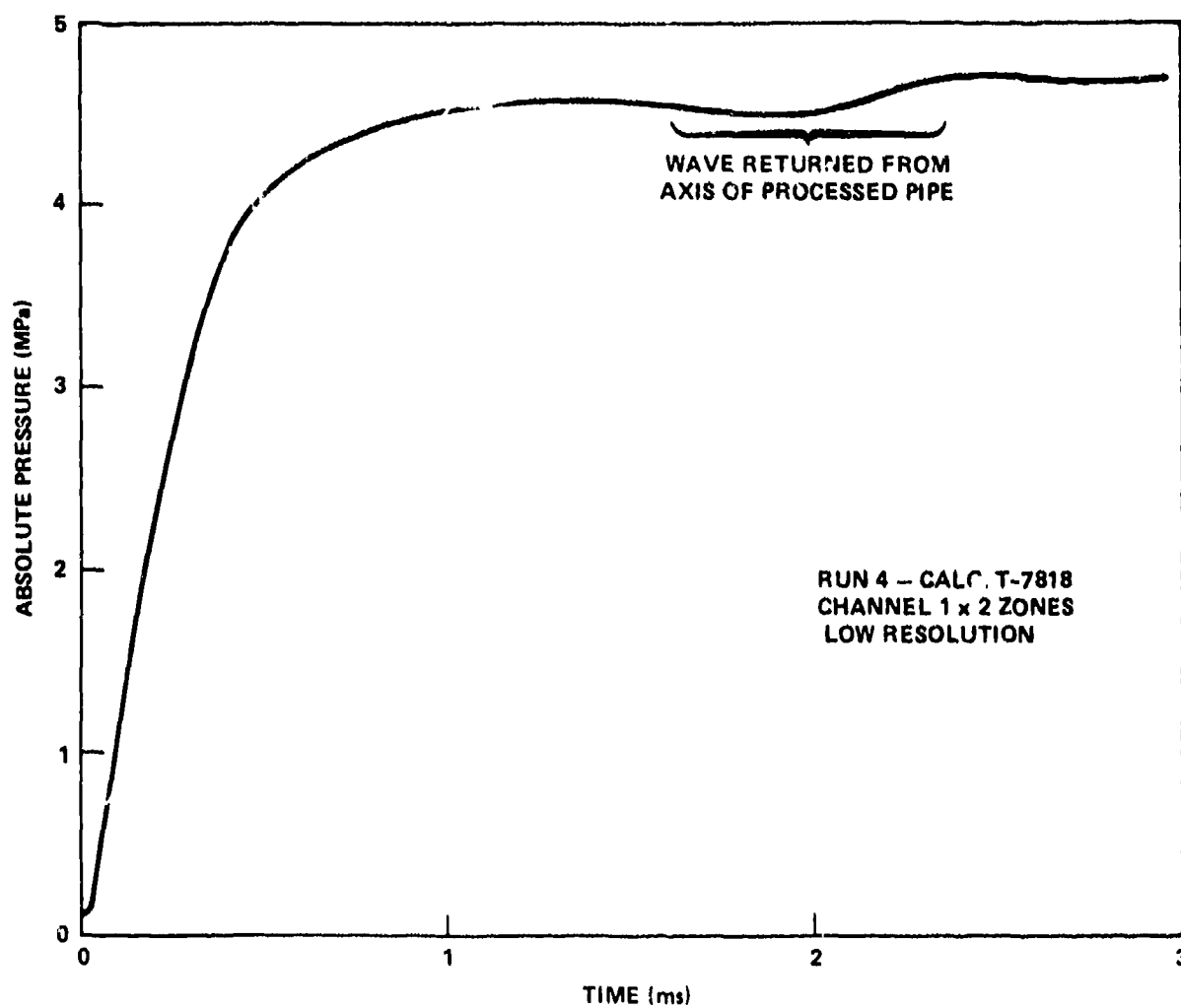FIGURE 6. PHENOMENA DURING STEAM OUTFLOW

FIGURE 7. EFFECT OF AXIAL REFLECTION OF RAREFACTION WAVE IN PROCESS PIPE
ON GUARD PIPE PRESSURE

and into the break. The net effect on the guard pipe reflected pressure loading is a negligible pressure oscillation that arrives after an essentially steady flow pattern at the guard pipe wall has been attained. The shape of the pressure oscillation indicated in Figure 7 represents the interaction of the rarefaction wave with the stationary shock and the guard pipe wall -- the lack of definition of this pressure oscillation is caused by the coarse zone size used in this computation.

SONIC FLOW IN PROCESS PIPE BREAK. Within the break, sonic flow conditions occur at the minimum flow cross section if the downstream pressure, p_d, is

$$p_d < p_u\left(\frac{2}{\gamma+1}\right)^{\frac{\gamma}{\gamma-1}}$$

where p_u is the upstream (reservoir) pressure and γ is the specific heat ratio of the gas.

For a free jet, the downstream pressure is equal to the ambient pressure. For a confined jet such as discussed here, the downstream pressure is not defined a priori because of the pressure buildup in the confined space. This does not present a problem for the hydrocode calculation because it automatically simulates the correct flow, whether it is sonic or subsonic. However, if preliminary hydrocode calculations indicate that the flow in the break remains sonic for the duration under investigation (which turns out to be the situation here), then considerable savings in computer costs can be made by assigning the proper steady flow conditions at the break exit and calculating only the flow downstream of the break for the various pipe spacings. The downstream flow cannot send any signals through the sonic flow into the process pipe.

DISCHARGE COEFFICIENT FOR PROCESS PIPE BREAK. The process pipe break is expected to have sharp edges. For such a "nozzle," the flow contracts and does not fill the "nozzle" cross section (Figure 8). This effect is the familiar vena contracta of incompressible flow and is known to occur for compressible flow as well (References 7 - 11). The area contraction

[7]Bean, H. S., Buckingham, E. and Murphy, P. S., "Discharge Coefficients of Square-Edged Orifices for Measuring the Flow of Air," N.B.S.J. Res. 2, pp 561-568, 1969.

[8]Stanton, T. E., "On the Flow of Gases at High Speeds," Proc. Roy. Soc. 111, pp 306-339, 1926.

[9]Perry, J. A., Jr., "Critical Flow Through Sharp-Edged Orifices," Trans. Am. Soc. Mech. Engrs. 71, pp 757-764, 1949.

[10]Grace, H. P. and Lapple, C. E., "Discharge Coefficients of Small-Diameter Orifices and Flow Nozzles," Trans. ASME, pp 639-647, Jul 1951.

[11]Arnberg, B. T., "Review of Critical Flowmeters for Gas Flow Measurements," J. Basic Engg., pp 447-461, Dec 1962.

NOZZLE WITH ROUNDED INLET

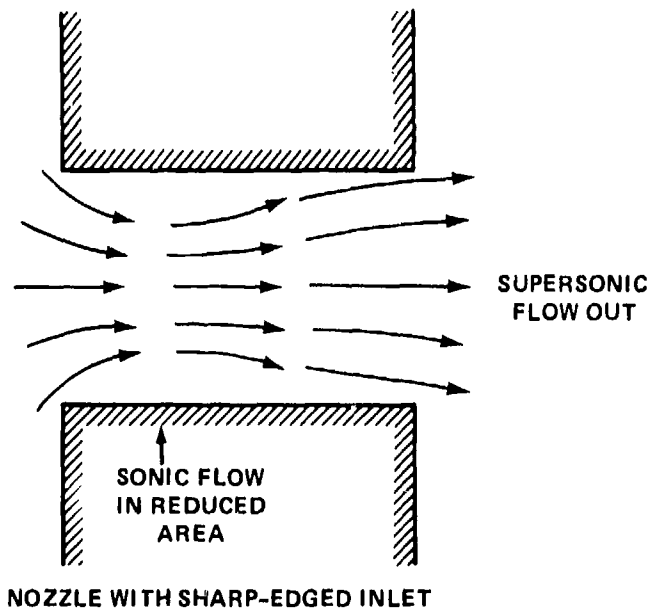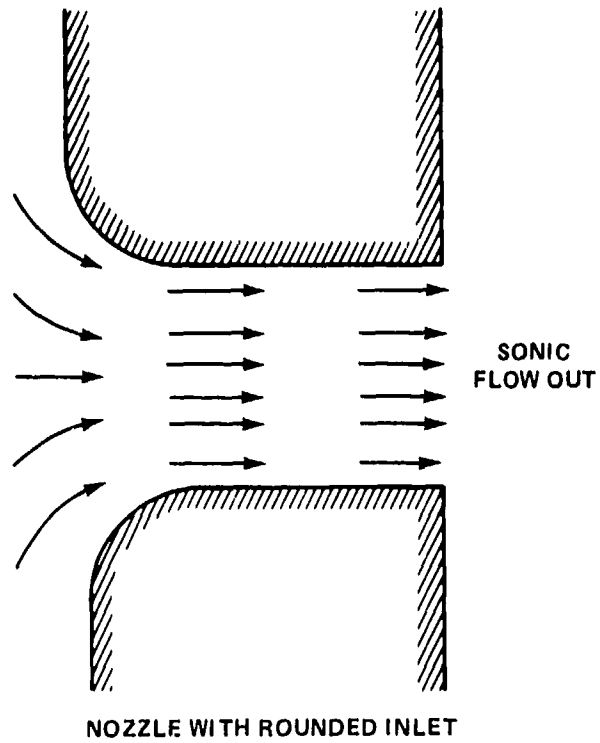NOZZLE WITH SHARP-EDGED INLET

FIGURE 8. ROUNDED VS SHARP-EDGED INLET

coefficient is typically between 0.6 and 1.0. This contraction allows the
downstream pressure to have some influence on the outflow even though the flow
is sonic, because signals can reach the sonic region by bypassing the sonic
core of the flow. Because no data were available on the flow of steam through
sharp-edged channels, the "nozzle" or process pipe break flow was determined
as part of the problem. The hydrocode calculations gave a discharge
coefficient of 0.77, compared with 1.00 expected for a rounded-inlet orifice.
This discharge coefficient is used in calculating the outflow from the process
pipe break exit for some of the truncated flow field calculations.

The steam jet reaches the end of the 50.8 mm (2.00 in) long break (process
pipe wall thickness) before the flow has expanded to fill the entire cross-
sectional area for the 50.8 mm break width. This result is evident in Table 3
which gives the steady-state outflow parameters, computed using CSQ, for the
8.3 MPa (1200 psia) process pipe reservoir conditions. The mass flux near the
centerline is 30% greater than the mass flux near the "nozzle" wall. The
effect is also indicated schematically in Figure 8 for the "nozzle" with the
sharp-edged inlet -- the figure indicates that the supersonic flow has not
expanded to encompass the entire area of the "nozzle," Results such as given
in Table 3 will be used to avoid calculation in every computer run of the
interior of the process pipe and the interior of the break.

TRUNCATED FLOW FIELD CALCULATIONS. To reduce computer time costs, the
runs with 8.3 MPa (1200 psia) process pipe reservoir conditions (Table 1,
Runs No. 1 - 12, 16, 17), were computed using a truncated flow field. The
calculation of the flow in the interior of the process pipe (the reservoir)
and the interior of the break (the "nozzle") was replaced by the steady-state
flow conditions of Table 3 at the break outlet since the effect of the rare-
faction wave moving into the reservoir was shown to be negligible in Figure 7.

For the 12.7 mm (0.5 in) wide breaks in these runs, the flow filled the
break exit, so the exit conditions were obtained from analytical sonic flow
calculations over 0.77 (the discharge coefficient determined for these sharp-
edged breaks or "nozzles") of the break area expanded to the full exit area
with the usual shock-tube area relations. The sonic conditions given in the
last line of Table 3 apply across the entire exit plane of the 12.7 mm (0.5 in)
wide breaks.

4.2 PRESSURES ON GUARD PIPE WALL

AIRSHOCK FORMATION BETWEEN PIPES. The exiting steam jet drives the air
between the pipes ahead of it, and forms at first a bow airshock at the nose
of the steam plume, and later an airshock that propagates ahead of the steam
jet flow in the space between the pipes.

Figure 9 presents a typical pressure distribution along the guard pipe
inside wall showing the presence of the airshock. The airshock shown in
the figure has an overpressure of 0.5 to 1.0 MPa (5 to 10 bars) and is not
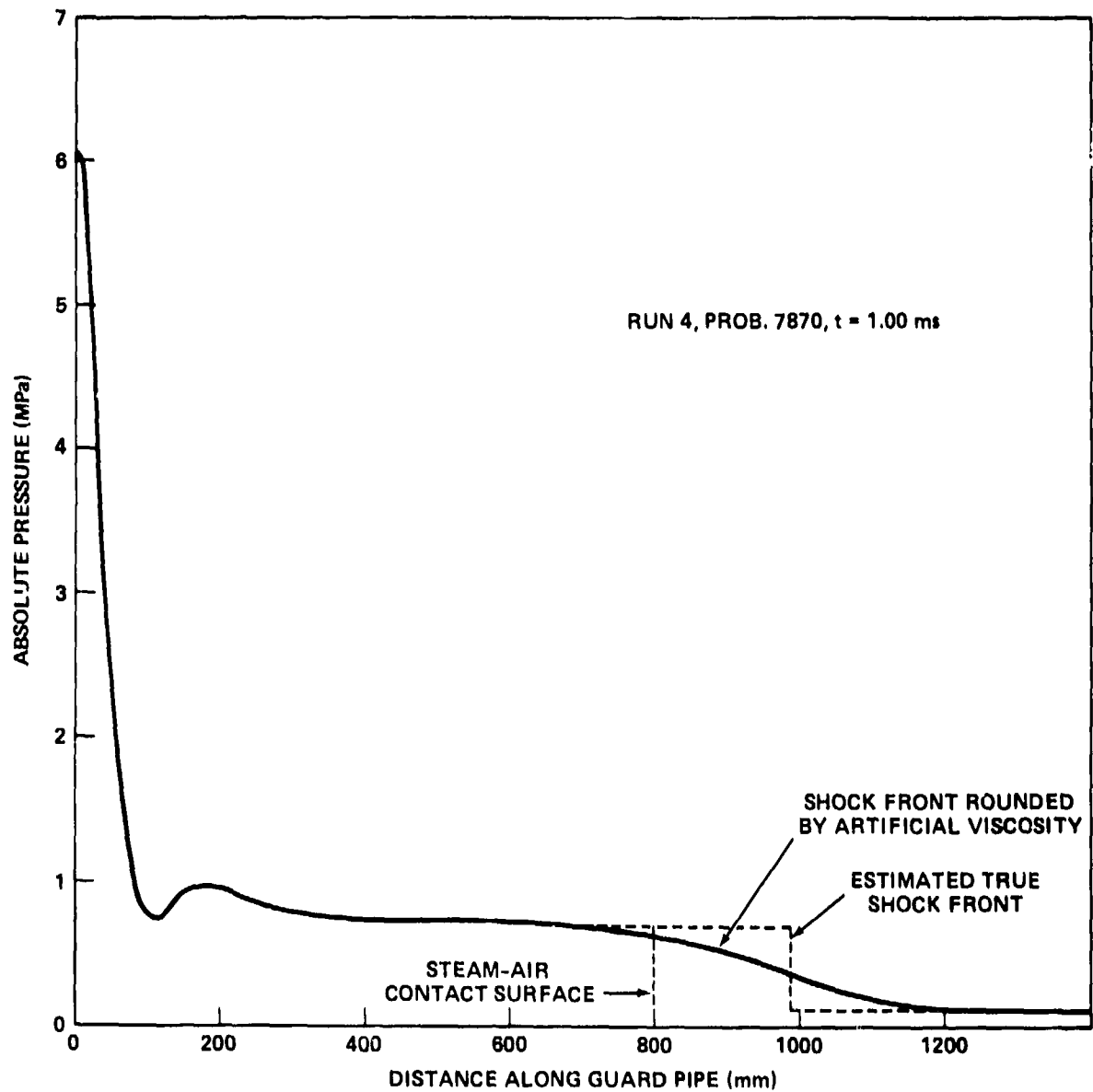regarded as structurally significant; it is therefore handled with coarse
zoning.

FIGURE 9. PRESSURE DISTRIBUTION ALONG GUARD PIPE, INCLUDING AIR SHOCK

In the remainder of this report, the discussion concentrates on the sharp pressure maximum on the guard pipe inside surface facing the site of the process pipe break.

PRESSURE TRANSIENTS ON THE GUARD PIPE WALL. Before discussing the main results, the pressure transients due to shock reflections between the oncoming steam jet and the guard pipe are examined briefly. These are poorly resolved in the two-dimensional calculations (e.g., see the oscillations in Figure 5). To resolve these shocks, the zoning scale would have to be about an order of magnitude finer and the computer cost for a two-dimensional calculation would be quite high. However, an upper bound can be obtained with a finely-zoned one-dimensional (WUNDY code; Reference 12) Lagrangean calculation. The simple linear shock tube geometry and the relationship with the geometry of the real problem are shown in Figure 10. The resulting pressure-time record at the guard pipe is shown in Figure 11. The reflected shocks are not significant because:

1) They are very short (about 10 μs) and carry little impulse;

2) They would be reduced by the two-dimensional expansion for the real problem geometry;

3) They would be very much reduced in amplitude by the finite opening time of the process pipe break which is assumed to be instantaneous for these calculations.

The opening time of a circumferential 50.8 nm (2.00 in) break in an infinite pipe with the parameters of Runs 1 through 12 is about 27 ms (Appendix A); the opening time of a longitudinal break is about 8 ms, calculated using a clamshell-type opening model with hinging at the side opposite the break.

These long opening times mean that the steam jet that first reaches the guard pipe originated from a small slit and would be greatly attenuated in pressure because the distance to the guard pipe would represent many slit widths.

These insignificant transient effects were ignored. The computational effort was directed towards determining the steady-state pressure distribution on the guard pipe. The slit (process pipe break exit) was assumed to open instantaneously, which allowed rapid attainment of the same steady flow that would have been eventually reached with a slowly-opening slit.

The steady-flow pressures reported in the next section represent over-estimates if the pipes are so short that the supply pressure drops before steady flow is attained.

---

[12] Lehto, D. and Lutzky, M., "One-Dimensional Hydrodynamic Code for Nuclear-Explosion Calculations," Naval Ordnance Laboratory, NOLTR 62-168, Mar 1965.
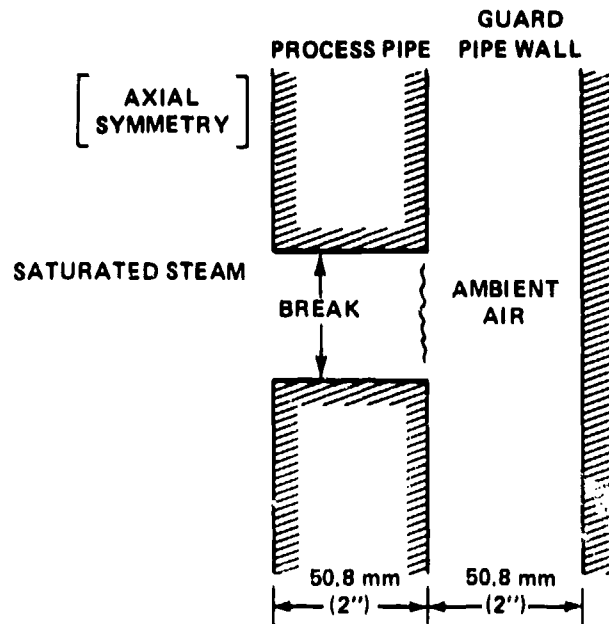
FIGURE 10a. GEOMETRY OF REAL PROBLEM
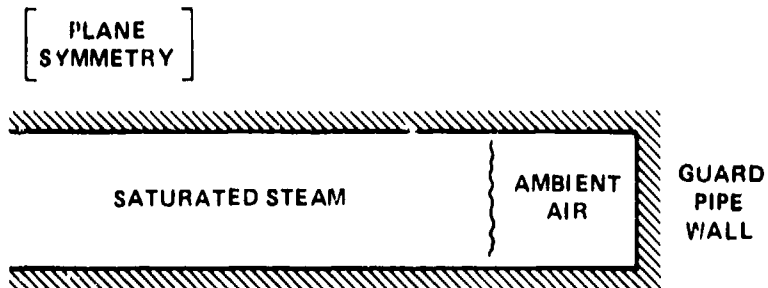
FIGURE 10b. GEOMETRY OF LINEAR SHOCK TUBE PROBLEM

29
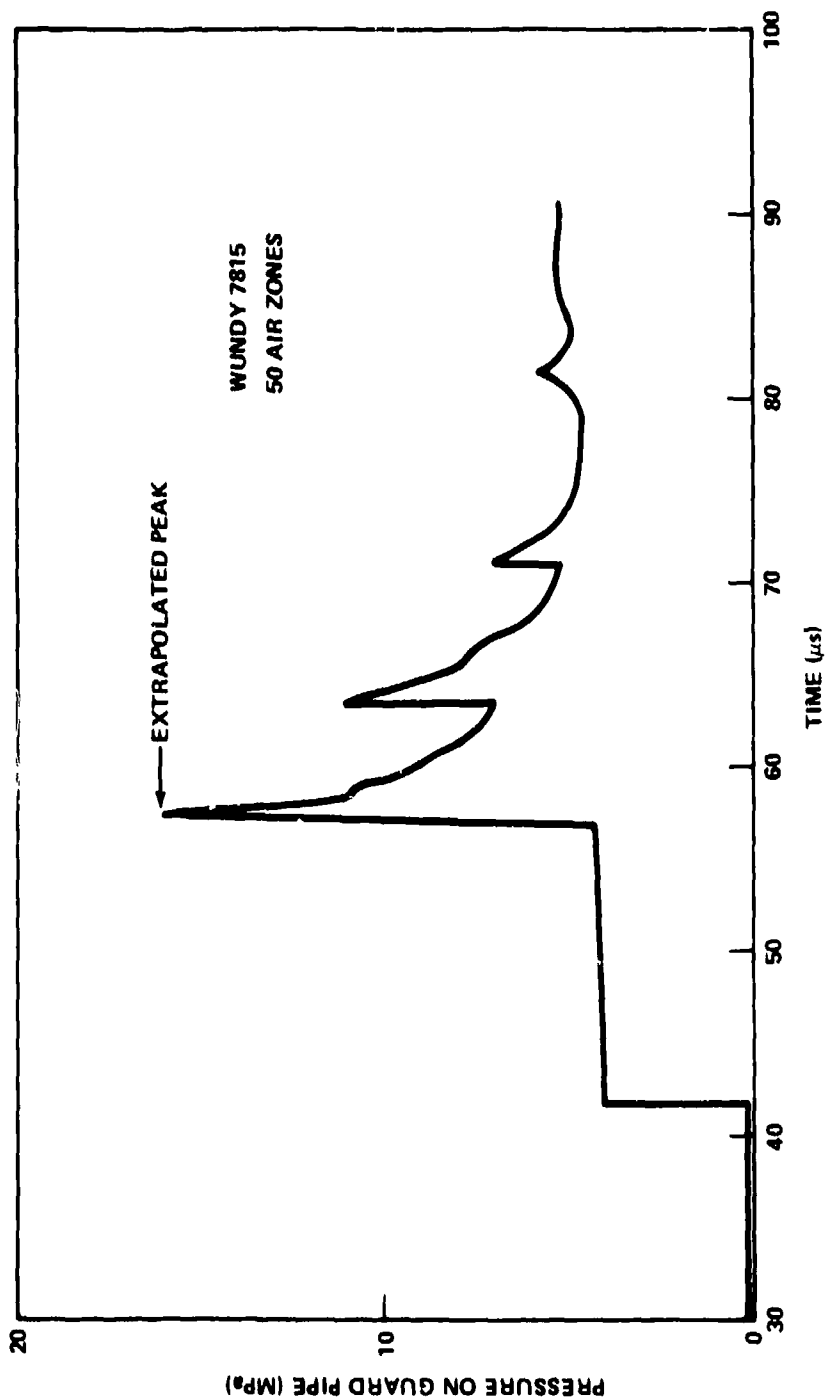
FIGURE 11. PRESSURE VS TIME ON GUARD PIPE FOR ONE-DIMENSIONAL FLOW

STEADY-FLOW PRESSURES ON GUARD PIPE WALL. The main results of this study are presented in Figures 12 - 15. These figures present the steady-flow pressure distribution on the guard pipe inside surface in the vicinity of the process pipe break. The full distribution of computed pressure data including the airshock effects are listed in corresponding Tables 4 - 6. The longitudinal-break maximum pressures are greater than the corresponding circumferential-break maximum pressures, because the latter flow has more geometric spreading (compare Figures 12 and 13 and see Figure 14).

In both process pipe break configurations, the maximum pressure drops off rapidly with increasing process/guard pipe separation distances.

A check was made on how the total force on the guard pipe plus the process pipe agrees with the thrust equation for a jet of outlet area A hitting an unconfined plate (Reference 1). Repeating the expression given in Chapter 2,

$$T/A_e = C_1 P_0 - P_\infty$$

with $C_1 = 1.229$ (for $\gamma = 1.1058$), $P_0 = 8.274$ MPa and $P_\infty = 0.101$ MPa

gives $T/A_e = 1.017 \times 10^8$ dyne/cm$^2 = 10.17$ N/m^2.

This can be compared with the net outward force on both pipes for the parallel-plate model of the longitudinal break:

$$F_{out} = \int_{gp} P_{gp} dA - \int_{pp} P_{pp} dA$$

For small plate separations, this integration removes most of the effect of the shock running between the plates, because the shock pressure distributions are nearly identical on the two surfaces. For large plate separations, the shock contribution does not cancel.

Figure 16 shows that the calculated net forces are close to those of the thrust equation. These integrals should not be regarded as precise, because they depend strongly on results in the rather coarsely zoned airshock region.

31

FIGURE 12. STEADY-FLOW PRESSURE ALONG GUARD PIPE FOR 50.8 mm (2 in)
CIRCUMFERENTIAL BREAK

FIGURE 13. STEADY-FLOW PRESSURE ALONG GUARD PIPE FOR 50.8 mm (2 in)
LONGITUDINAL BREAK

FIGURE 14. STEADY-FLOW PRESSURE ALONG GUARD PIPE FOR 12.7 mm (0.5 in)
CIRCUMFERENTIAL AND LONGITUDINAL BREAKS

FIGURE 15. STEADY-FLOW PRESSURE ALONG GUARD PIPE FOR MISCELLANEOUS RUNS 13, 14, 15

TABLE 4
STEADY FLOW PRESSURES ALONG INSIDE OF GUARD PIPE DUE TO STEAM JET FROM 50.8 MM (2 IN) BREAK IN PROCESS PIPE

0.914 M (36 IN) O.D. PROCESS PIPE
8.274 MPA (1200 PSIA) SATURATED STEAM

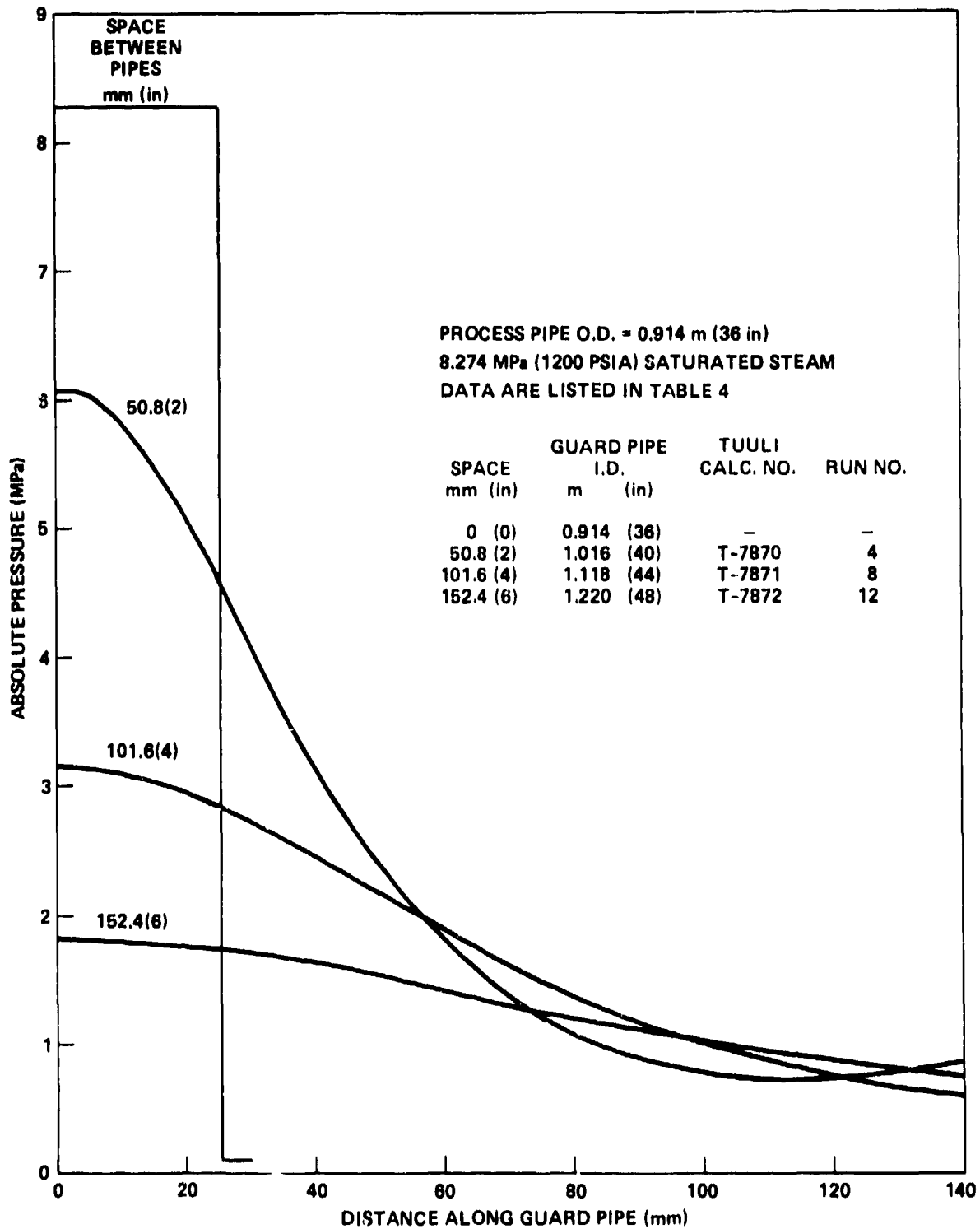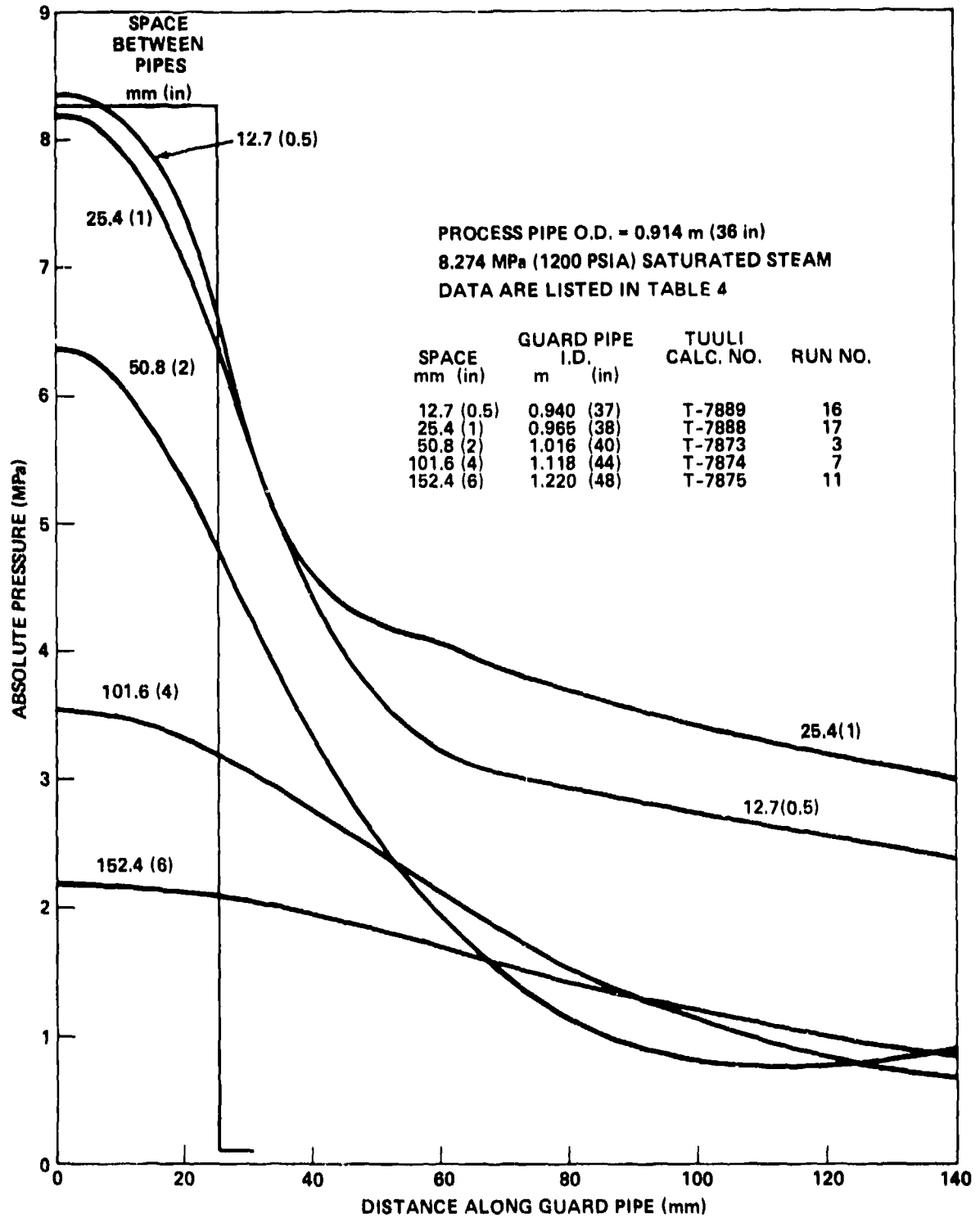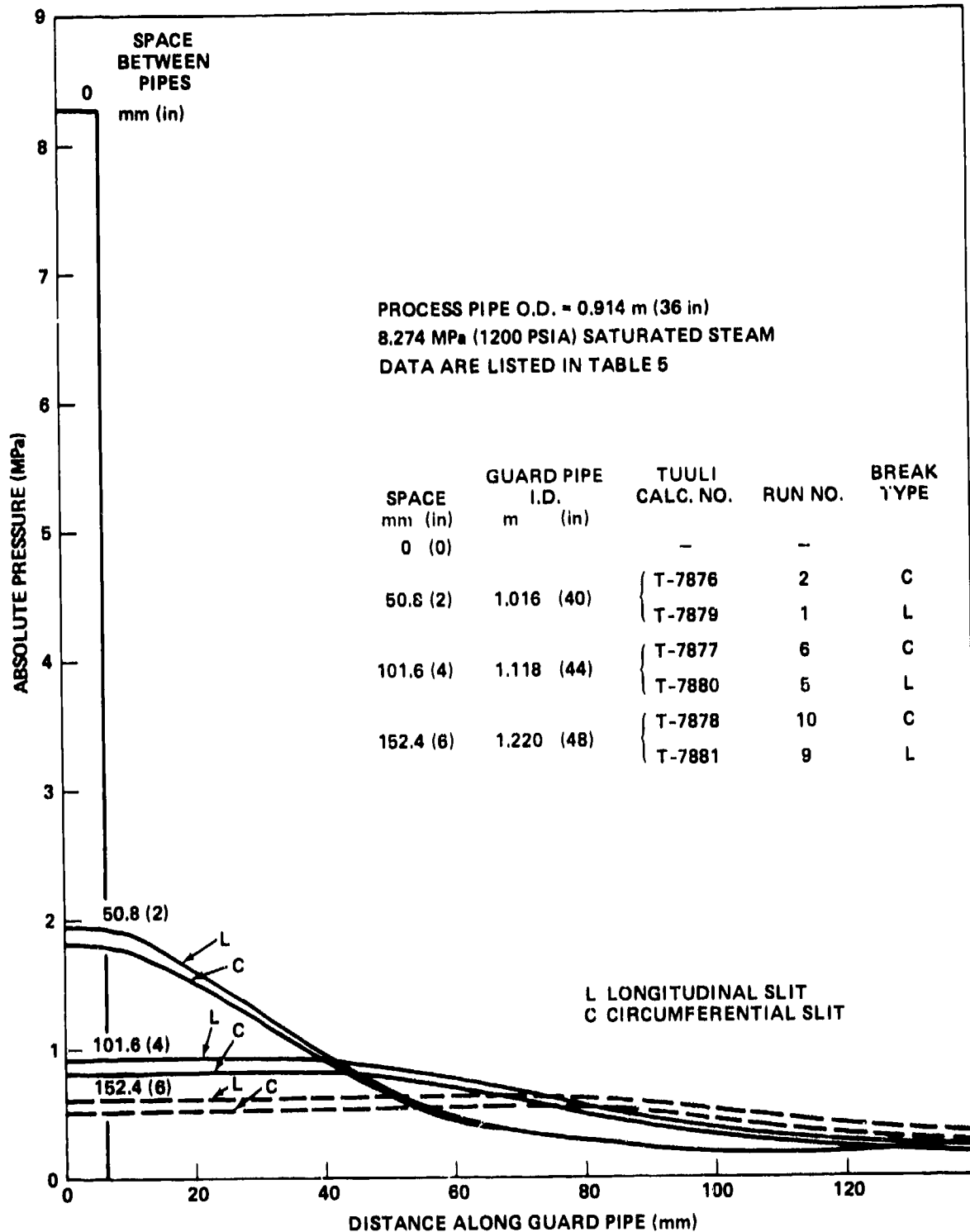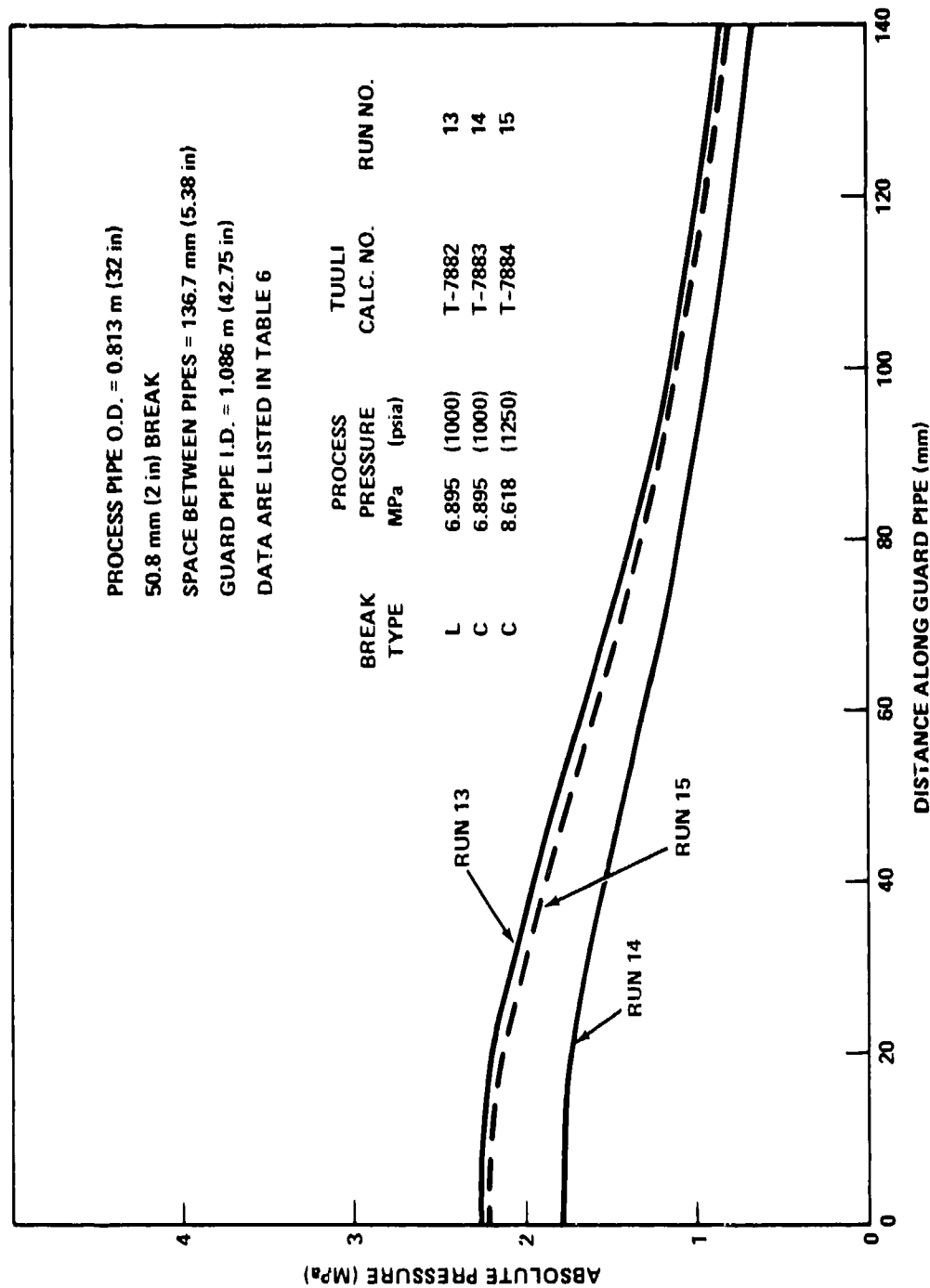Z=DISTANCE ALONG GUARD PIPE FROM CENTER OF BREAK (MM).
P=ABSOLUTE PRESSURE ON GUARD PIPE (MPA).
SPACE=SPACE BETWEEN PIPES (MM).
AMBIENT PRESSURE IS 0.101 MPA (14.70 PSI).

	CIRCUMFERENTIAL BREAK			LONGITUDINAL BREAK				
PROB.NO.	7870	7871	7872	7884	7888	7873	7874	7875
SPACE	50.8	101.6	152.4	12.7	25.4	50.8	101.6	152.4
Z	P	P	P	P	P	P	P	P
1.6	6.06	3.14	1.82	8.36	8.19	6.34	3.53	2.16
4.8	6.05	3.14	1.80	8.16	8.18	6.33	3.53	2.19
8.0	5.92	3.12	1.80	8.27	8.05	6.20	3.51	2.19
11.2	5.77	3.10	1.81	8.14	7.90	6.05	3.48	2.18
14.3	5.57	3.06	1.80	7.97	7.67	5.85	3.44	2.16
17.5	5.31	3.00	1.79	7.72	7.37	5.59	3.38	2.15
20.7	5.03	2.95	1.77	7.37	7.01	5.30	3.31	2.13
23.9	4.72	2.87	1.75	6.94	6.58	4.97	3.23	2.10
27.0	4.39	2.80	1.74	6.29	6.13	4.63	3.15	2.08
30.3	4.04	2.71	1.71	5.67	5.64	4.28	3.05	2.05
34.0	3.68	2.62	1.69	5.12	5.15	3.90	2.95	2.02
38.0	3.30	2.51	1.64	4.71	4.66	3.51	2.82	1.97
42.5	2.92	2.39	1.61	4.44	4.20	3.10	2.69	1.93
47.5	2.55	2.25	1.56	4.26	3.82	2.72	2.53	1.87
52.5	2.23	2.11	1.50	4.18	3.52	2.37	2.37	1.80
57.5	1.94	1.96	1.45	4.10	3.31	2.07	2.21	1.73
62.5	1.70	1.83	1.39	4.01	3.16	1.81	2.05	1.66
67.5	1.48	1.69	1.33	3.92	3.07	1.58	1.90	1.58
72.5	1.30	1.55	1.27	3.82	3.00	1.39	1.74	1.51
78.5	1.11	1.40	1.21	3.72	2.94	1.18	1.58	1.43
86.0	.951	1.25	1.14	3.61	2.88	1.01	1.40	1.34
95.0	.815	1.09	1.07	3.49	2.80	.865	1.22	1.25
106.0	.731	.931	.983	3.36	2.69	.771	1.04	1.13
119.0	.729	.759	.884	3.22	2.55	.765	.864	1.01
131.0	.437	.611	.772	3.05	2.42	.878	.686	.883
138.0	.944	.479	.655	2.88	2.26	.994	.537	.749
165.0	.954	.372	.535	2.68	2.10	1.01	.412	.612
200.0	.402	.309	.421	2.45	1.91	.949	.332	.481
265.0	.625	.332	.338	2.22	1.72	.864	.342	.379
325.0	.711	.416	.306	1.97	1.52	.802	.434	.321
415.0	.735	.459	.380	1.71	1.32	.760	.482	.385
525.0	.714	.493	.439	1.50	1.18	.734	.510	.462
635.0	.700	.511	.406	1.35	1.09	.716	.535	.448
745.0	.656	.437	.292	1.25	1.04	.703	.479	.344
860.0	.596	.269	.165	1.16	.964	.621	.309	.200
980.0	.355	.147	.112	1.08	.790	.416	.166	.122
1100.0	.157	.107	.102	.900	.479	.204	.111	.103
1230.0	.111	.101	.101	.477	.186	.117	.102	.101
1370.0	.102	.101	.101	.174	.109	.102	.101	.101
1520.0	.101	.101	.101	.107	.101	.101	.101	.101

TABLE 5
STEADY FLOW PRESSURES ALONG INSIDE OF GUARD PIPE DUE TO STEAM JET FROM 12.7 MM (0.5 IN) BREAK IN PROCESS PIPE

0.914 M (36 IN) O.D. PROCESS PIPE
8.274 MPA (1200 PSIA) SATURATED STEAM

Z=DISTANCE ALONG GUARD PIPE FROM CENTER OF BREAK (MM).
P=ABSOLUTE PRESSURE ON GUARD PIPE (MPA).
SPACE=SPACE BETWEEN PIPES (MM).
AMBIENT PRESSURE IS 0.101 MPA (14.70 PSI).

	CIRCUMFERENTIAL BREAK			LONGITUDINAL BREAK		
PROB.NO.	7876	7877	7878	7879	7880	7881
SPACE	50.8	101.6	152.4	50.8	101.6	152.4
Z	P	P	P	P	P	P
.8	1.79	.815	.518	1.93	.922	.611
2.4	1.80	.815	.517	1.93	.923	.612
4.0	1.81	.814	.517	1.94	.926	.611
5.6	1.80	.813	.516	1.94	.924	.610
7.2	1.80	.814	.516	1.93	.924	.611
8.7	1.78	.813	.516	1.91	.924	.610
10.3	1.76	.816	.516	1.89	.928	.611
11.9	1.73	.815	.515	1.85	.926	.610
13.6	1.69	.819	.516	1.81	.930	.612
15.4	1.65	.817	.515	1.76	.929	.612
17.7	1.59	.823	.516	1.70	.934	.614
20.5	1.51	.821	.516	1.60	.932	.614
24.0	1.41	.828	.520	1.49	.937	.619
28.0	1.29	.828	.522	1.35	.934	.621
32.0	1.16	.829	.526	1.20	.931	.626
36.0	1.03	.824	.530	1.07	.922	.628
40.0	.913	.816	.534	.942	.908	.633
44.0	.799	.802	.538	.824	.889	.634
48.0	.692	.779	.543	.716	.861	.637
52.5	.584	.753	.545	.607	.828	.638
58.5	.474	.714	.557	.496	.784	.643
66.0	.378	.643	.558	.399	.709	.638
75.0	.296	.552	.556	.315	.613	.628
86.0	.231	.449	.524	.249	.506	.596
99.0	.189	.350	.461	.204	.401	.536
114.0	.177	.266	.381	.192	.310	.456
131.0	.231	.201	.303	.230	.236	.370
150.0	.282	.157	.236	.298	.181	.293
172.0	.338	.132	.183	.350	.144	.225
200.0	.361	.141	.149	.369	.136	.175
232.0	.368	.195	.141	.376	.179	.149
270.0	.375	.251	.182	.383	.245	.164
315.0	.388	.259	.240	.397	.276	.224
370.0	.399	.263	.279	.408	.273	.277
440.0	.404	.284	.290	.413	.291	.309
530.0	.427	.285	.226	.436	.298	.260
640.0	.396	.203	.143	.413	.216	.163
750.0	.221	.122	.107	.237	.127	.111
940.0	.124	.103	.101	.129	.104	.102
1100.0	.103	.101	.101	.104	.101	.101

TABLE 6

STEADY FLOW PRESSURES ALONG INSIDE OF GUARD PIPE DUE TO STEAM JET FROM BREAK IN PROCESS PIPE

Z=DISTANCE ALONG GUARD PIPE FROM CENTER OF BREAK (MM).
P=ABSOLUTE PRESSURE ON GUARD PIPE (MPA).
PU=PRESSURE IN PROCESS PIPE (MPA).
PROCESS PIPE DIAMETER = 812.8 MM (32 IN).
GUARD PIPE DIAMETER = 1086. MM (42.75 IN).
AMBIENT PRESSURE   = 0.101 MPA (14.70 PSI).

PROB.NO.	7882	7883	7884
BREAK TYPE	CIRC	LONG	LONG
PU	6.895	6.895	8.618
Z	P	P	P
1.6	2.26	1.78	2.21
4.8	2.26	1.78	2.21
8.0	2.26	1.78	2.21
11.2	2.25	1.77	2.20
14.4	2.23	1.75	2.18
17.6	2.21	1.74	2.15
20.8	2.18	1.71	2.12
23.9	2.15	1.69	2.09
27.0	2.11	1.66	2.05
30.3	2.07	1.63	2.01
34.0	2.02	1.59	1.96
38.5	1.96	1.54	1.89
44.5	1.88	1.48	1.81
53.0	1.77	1.39	1.69
64.0	1.61	1.27	1.54
77.5	1.42	1.13	1.36
95.0	1.22	.975	1.16
118.0	1.00	.800	.954
145.0	.801	.630	.752
180.0	.609	.477	.568
225.0	.461	.369	.431
280.0	.379	.325	.361
345.0	.375	.345	.366
420.0	.427	.402	.421
510.0	.488	.442	.475
620.0	.448	.368	.419
740.0	.309	.229	.277
865.0	.166	.130	.149
1000.0	.110	.104	.107
1140.0	.102	.101	.101
1260.0	.101	.101	.101
1420.0	.101	.101	.101
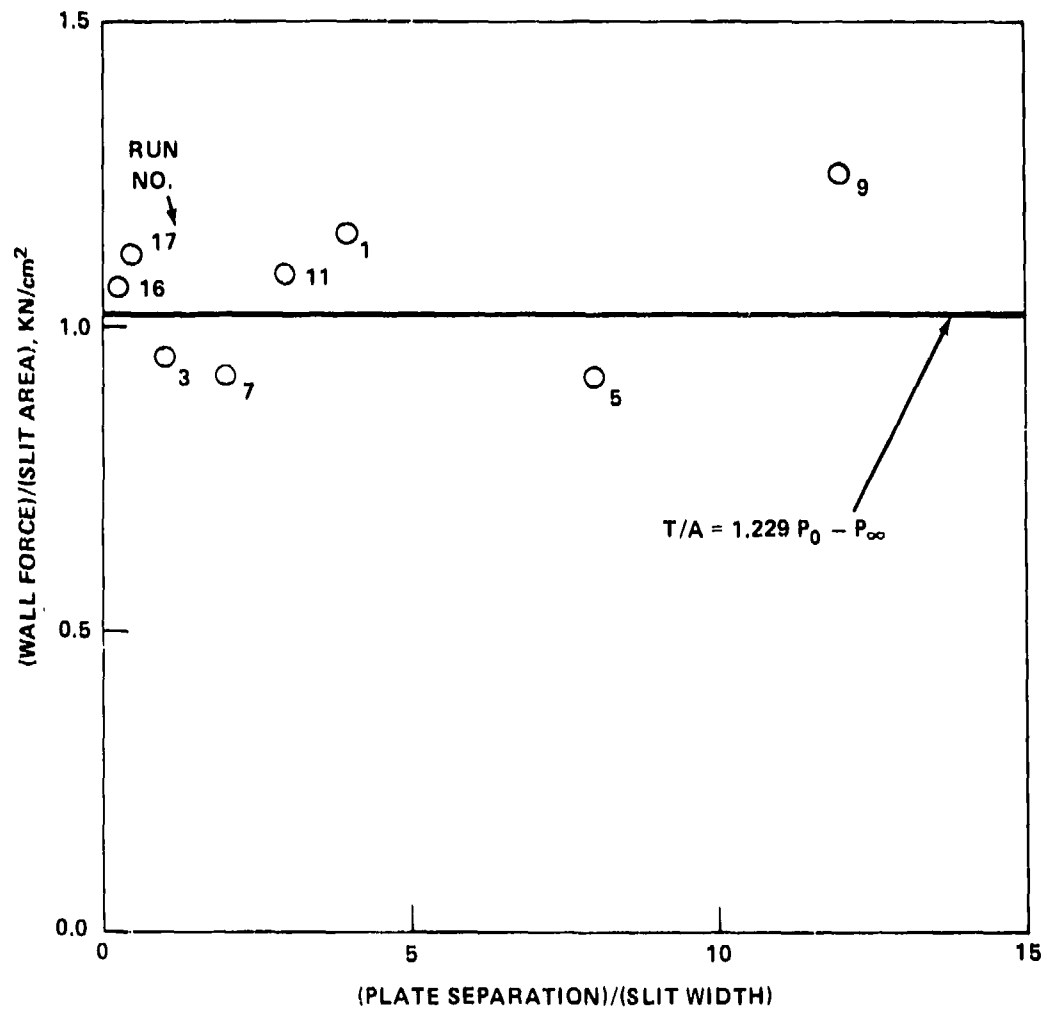
FIGURE 16. NET FORCES ON PLATES

Figure 17 shows the pressure distributions (indicating the presence of
the stationary shock) along the plane of symmetry passing through the center
of the longitudinal break for selected process/guard pipe separation distances.
The stationary shock (in the steam) shows the characteristic smoothing-out of
the discontinuity that is inherent in the artificial-viscosity method for
handling shock discontinuities numerically.

Some details cf the steady flow (for longitudinal-break configuration)
in Runs 7 and 11 are presented in Figures 18 and 19, respectively. These
runs differ only in the spacing between the pipes (4 and 6 inches, respectively).
The solid curves are isobars. There is a region of backflow towards the break
in both figures. The entire flow field in Figure 18 is composed of steam.
Figure 19 shows a trapped streamer of air, which conveniently delineates the
boundary of the steam jet.

FIGURE 17. STEADY-FLOW PRESSURE DISTRIBUTION ALONG PLANE OF SYMMETRY
FOR LONGITUDINAL 50.8 (2 in) BREAK
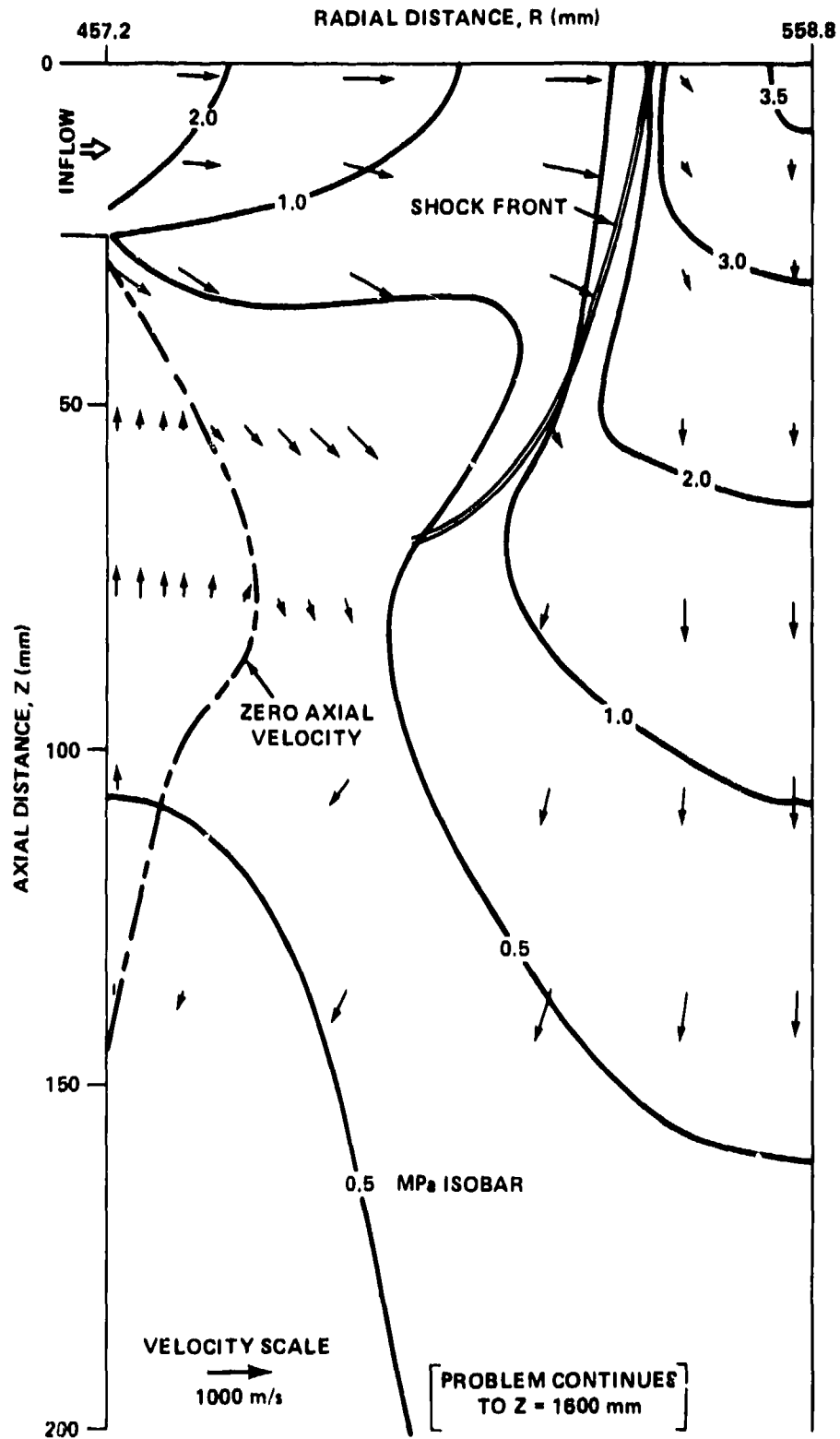
FIGURE 18. FLOW PATTERN FOR PROBLEM NO. 7874 (RUN 7)
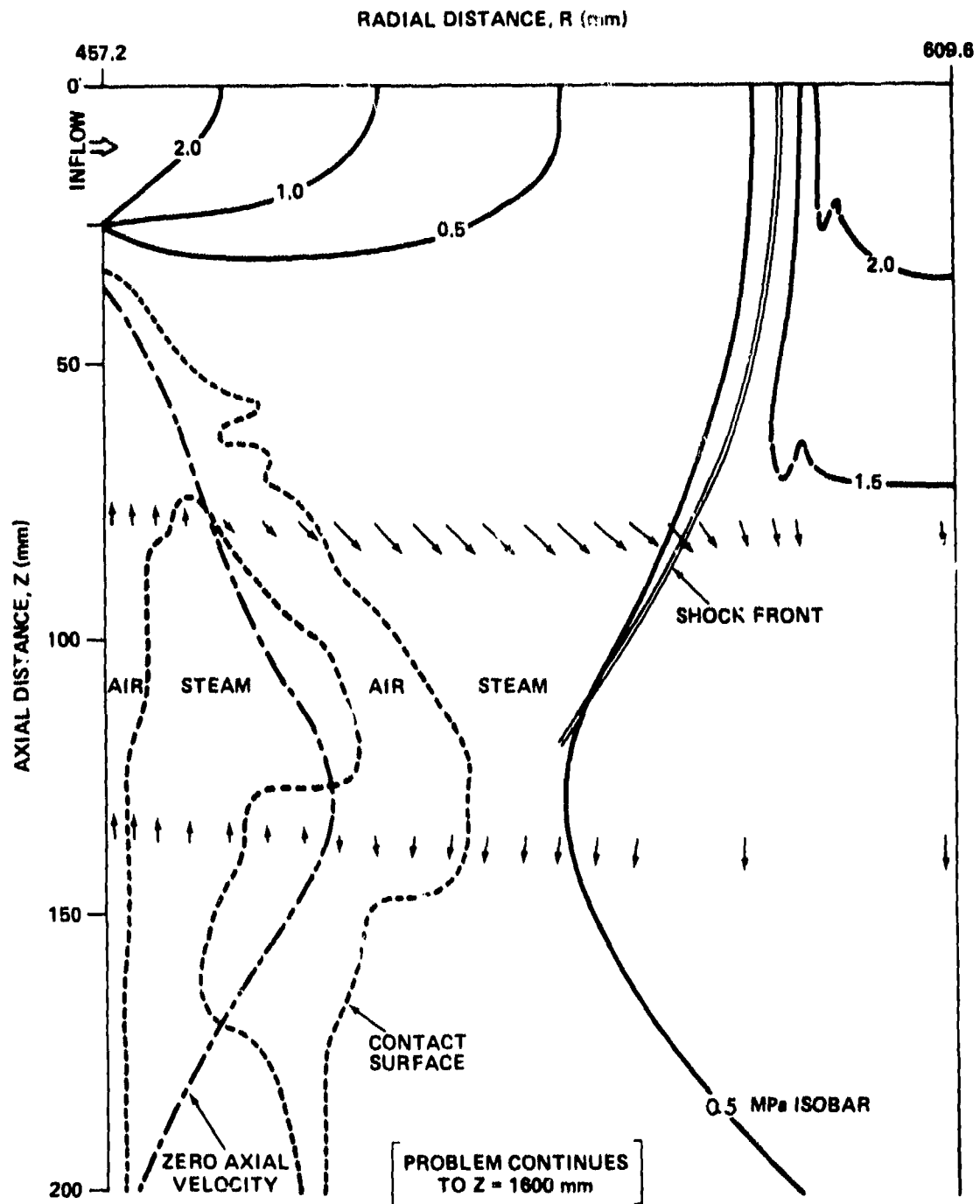
FIGURE 19. FLOW PATTERN FOR PROBLEM NO. 7875 (RUN 11)

CHAPTER 5

CONCLUSIONS

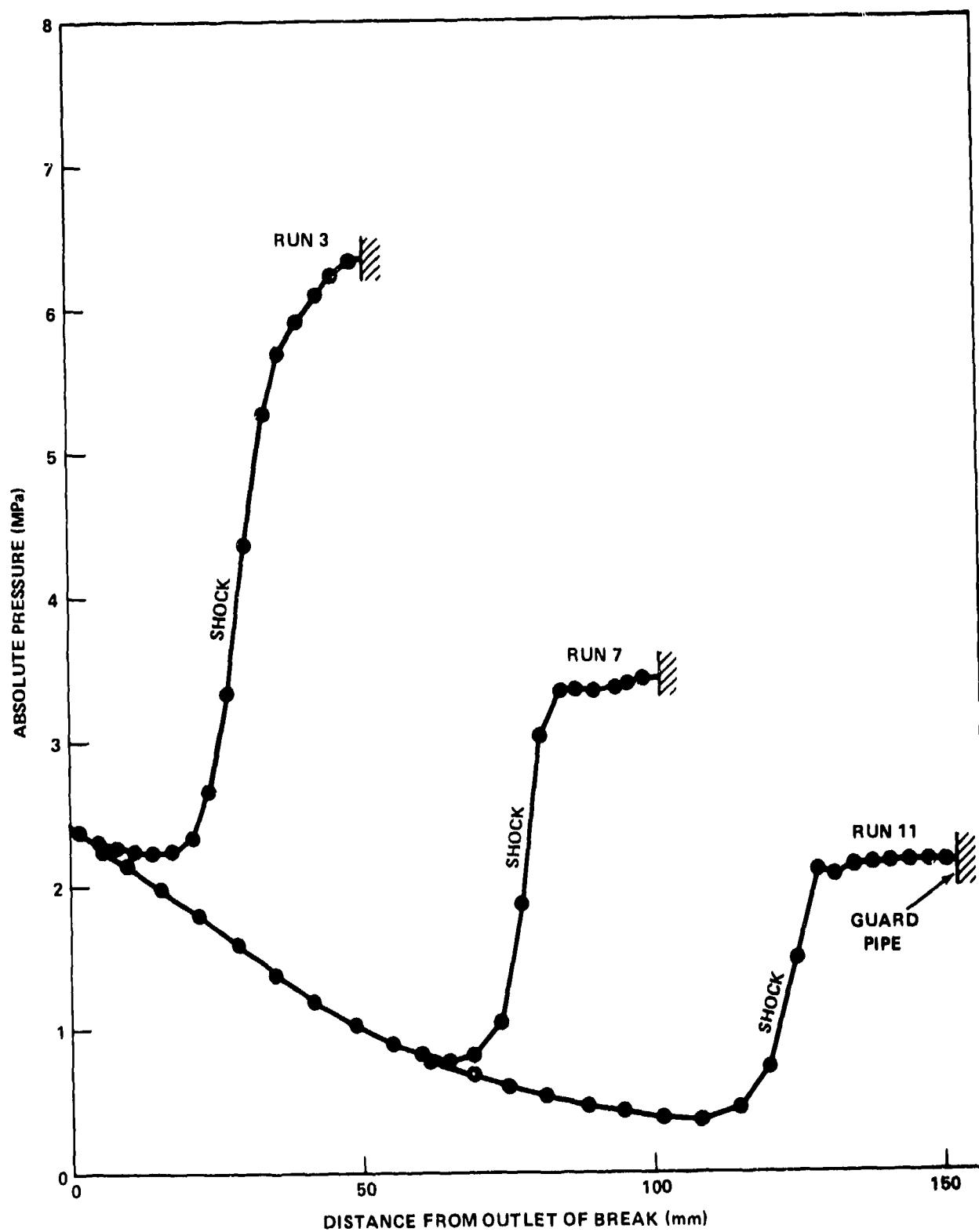The results in Figures 12 - 15 indicate that the steady-flow maximum pressure loads on the guard pipe inside surface produced by ruptures (longitudinal and circumferential) of the steam process pipe are less than the initial process pipe steam pressure (as Bernollis' law would indicate). As the process/guard pipe separation distance approaches zero the pressure loading approaches the initial process pipe steam pressure. The guard pipe pressure loads fall off rapidly with distance from the process pipe break site along the guard pipe surface. Transient airshocks with high peak pressures (and very short durations) occur before the flow becomes steady; however, these airshocks do not transmit sufficient momentum to the guard pipe wall to affect the guard pipe structural response appreciably. A guard pipe designed to withstand the process pipe pressure can withstand a steam jet from a break in the process pipe. The effect of whipping of the process pipe is not considered in this report.

Only simple size scaling can be accurately applied to these results (i.e., multiplying all dimensions and time by the same factor). The maximum pressure on the guard pipe depends strongly on the ratio of distance to guard pipe divided by break width, and weakly on the ratio of break length (i.e., pipe thickness) to break width and on the equation of state for steam.

REFERENCES

1. Moody, F. J., "Prediction of Blowdown Thrust and Jet Forces," ASME Paper 69-HT-31, ASME-AIChE Heat Transfer Conference, Minneapolis, Minn., Aug 1969.

2. Gentry, R. A., Martin, R. E., and Daly, B. J., "An Eulerian Differencing Method for Unsteady Compressible Flow Problems," J. Comput. Phys. 1, pp 87-118, 1966.

3. Thompson, S. L., "CSQ--A Two Dimensional Hydrodynamic Program with Energy Flow and Material Strength," Sandia Labs. SAND 74-0122, Aug 1975.

4. Keenan, J. H. and Keyes, F. G., Thermodynamic Properties of Steam, Including Data for the Liquid and Solid Phases, 1st ed., Wiley, New York, 1936.

5. Zel'dovich, Ya. B. and Raizer, Yu. P., Physics of Shock Waves and High Temperature Hydrodynamic Phenomena, Volume II, ed. by W. D. Hayes and R. F. Probstein, Academic Press, New York, 1967.

6. Kreith, F., Principles of Heat Transfer, 2nd ed., International Textbook Co., Scranton, Pa., 1965.

7. Bean, H. S., Buckingham, E. and Murphy, P. S., "Discharge Coefficients of Square-Edged Orifices for Measuring the Flow of Air," N. B. S. J. Res. 2, pp 561-568, 1969.

8. Stanton, T. E., "On the Flow of Gases at High Speeds," Proc. Roy. Soc. 111, pp 306-339, 1926.

9. Perry, J. A., Jr., "Critical Flow Through Sharp-Edged Orifices," Trans. Am. Soc. Mech. Engrs. 71, pp 757-764, 1949.

10. Grace, H. P. and Lapple, C. E., "Discharge Coefficients of Small-Diameter Orifices and Flow Nozzles," Trans. ASME, pp 639-647, Jul 1951.

11. Arnberg, B. T., "Review of Critical Flowmeters for Gas Flow Measurements," J. Basic Engg., pp. 447-460, Dec 1962.

12. Lehto, D. and Lutzky, M., "One-Dimensional Hydrodynamic Code for Nuclear-Explosion Calculations," Naval Ordnance Laboratory, NOLTR 62-168, Mar 1965.

A1. Kolsky, H., Stress Waves in Solids, Dover, New York, 1963.

A2. Gray, D. E. (ed.), American Institute of Physics Handbook, 3rd ed., McGraw-Hill, 1972.

APPENDIX A

OPENING TIME OF CIRCUMFERENTIAL BREAK IN PROCESS PIPE

Assume that the break occurs instantaneously and calculate how long it takes for the ends to pull apart to the desired break size. The mechanism for pulling the ends apart is a relief wave that propagates along the pipe and drops the meridional stress from its loaded condition to zero stress. The meridional stress is

$$\sigma = \frac{pR}{2t} = \underline{36.20 \text{ MPa}} = \underline{5250 \text{ psi}}$$

where   p = pressure in pipe (=8.274 MPa = 1200 psia)

R = radius of pipe (=0.445m = 17.5 in)

t = thickness of pipe (=50.8 mm = 2 in)

The speed of a longitudinal wave in an infinite plate is (Reference A1 - p. 81)

$$c_L = \sqrt{\frac{E}{\rho(1-\nu^2)}} = \underline{5.24 \times 10^3 \text{ m/s}}$$

where   E = Young's modulus   (=2.0 × 10^5 MPa for steel (Reference A2 - p. 2-68))

ν = Poisson's ratio   (=0.3)

ρ = density   (=8 × 10^3 kg/m^3)

The speed of the pipe (particle velocity) in the stress-relieved region is

$$v = \left(\frac{\sigma}{E}\right) c_L = \underline{0.948 \text{ m/s}}$$

[A1] Kolsky, H., Stress Waves in Solids, Dover, New York, 1963.

[A2] Gray, D. E. (ed.), American Institute of Physics Handbook, 3rd ed., McGraw-Hill, 1972.

To open a 50.8 mm (2 in) break, each end has to move 25.4 mm (1 in). The time this takes is

$$t \text{ (25.4 mm = 1 in)} = \text{(25.4 mm)} / \text{(0.948} \times 10^3 \text{ mm/s)} = \underline{26.8 \text{ ms}}$$

In this time, the elastic relief wave has moved down the pipe a distance of (0.0268 s) x (5.24 x 10⁵ m/s) = 140 m. Anything within 70 m that inhibits longitudinal motion of the pipe would send back a wave that would slow the opening of the gap before it reached a total size of 50.8 mm (2 in).

DISTRIBUTION LIST

Copies

U. S. Nuclear Regulatory Commission
Washington, D. C. 20555
Attn: R. J. Bosnak (DSS) - P924   6
       H. L. Brammer (DSS) - P924   1
       S. N. Hou (DSS) - P924   1
       R. J. Mattson (DSS) - P1102   1
       J. J. Burns (RES) - 1130SS   3
       V. S. Noonan (EB) - 440   1

Defense Technical Information Center   12
Cameron Station
Alexandria, VA 22314

Library of Congress   4
Washington, D. C. 20540
Attn: Gift and Exchange Division

Commander   1
Field Command
Defense Nuclear Agnecy
Attn: FCTA
Kirtland Air Force Base, NM 87115

Battelle Memorial Institute   1
505 King Avenue
Columbus, OH 43201

Denver Research Institute   1
Mechanical Sciences and Environmental Engineering
University of Denver
Denver, CO 80210
Attn: J. Wisotski

Falcon Research   1
Denver, CO 80210
Attn: D. Parks

DISTRIBUTION LIST (Cont.)

Copies

General American Transportation Corporation
General American Research Division
7449 North Natchez Avenue
Niles, IL 60648   1
Attn: W. Byrne   1
       T. Schiffman

General Electric Company - Tempo   1
816 State Street
Santa Barbara, CA 93102
Attn: W. Chan/DASIAC

Hercules Incorporated   1
Box 98
Magna, UT 84044
Attn: D. Richardson

IIT Research Institute
10 West 35th Street
Chicago, IL 60616   1
Attn: Technical Library   1
       J. Dahn   1
       H. Napadensky

Institute for Defense Analysis   1
400 Army-Navy Drive
Arlington, VA 22202
Attn: Library

Kaman Sciences Corp.   1
P. O. Box 7463
Colorado Springs, CO 80907

Los Alamos Scientific Laboratory
P. O. Box 1663
Los Alamos, NM 87544   1
Attn: LASL Library   1
       C. Mader   1
       R. Rogers   1
       L. Smith

DISTRIBUTION LIST (Cont.)

Copies

New Mexico Institute of Mining and Technology
TERA
Socorro, NM 87801
Attn: M. L. Kempton   1
       J. P. McLain   1

Pacifica Technology   1
P. O. Box 148
Del Mar, CA 92014

Physics International Company
2700 Merced Street
San Leandro, CA 94577
Attn: D. Randall   1
       F. Sauer   1

Pittsburgh Mining and Safety Research Center
U. S. Bureau of Mines
4800 Forbes Avenue
Pittsburgh, PA 15213
Attn: R. Vandolah   1
       R. Watson   1

R and D Associates   1
P. O. Box 3580
Santa Monica, CA 90403
Attn: Technical Library

Sandia Laboratories
P. O. Box 5800
Albuquerque, NM 87115
Attn: Library   1
       J. Reed   1
       L. Vortman   1

Sandia Laboratories   1
Livermore Laboratory
P. O. Box 969
Livermore, CA 94550

DISTRIBUTION LIST (Cont.)

	Copies

Director
Scripps Institution of Oceanography
La Jolla, CA 92037

1

Shock Hydrodynamics Incorporated
15010 Ventura Boulevard
Sherman Oaks, CA 91403
Attn: L. Zernow

1

Southwest Research Institute
8500 Culebra Road
San Antonio, TX 78206
Attn: W. Baker
 R. White

1
1

Systems, Science and Software
P. O. Box 1620
La Jolla, CA 92037

1

University of California
Lawrence Livermore Laboratory
P. O. Box 808
Livermore, CA 94550
Attn: B. Dobratz
 M. Finger
 E. James
 J. Kury
 E. Lee

1
1
1
1
1

University of New Mexico
Eric H. Wang Civil Engineering Research Facility
University Station
Box 188
Albuquerque, NM 87131

1

URS Corporation
155 Bonet Road
San Mateo, CA 94402
Attn: Document Control

1

DISTRIBUTION LIST (Cont.)

Copies

Director Woods Hole Oceanographic Institute Woods Hole, MA 02543	1
Lovelace Foundation for Medical Education 5200 Gibson Blvd, S. E. Albuquerque, NM 87103	1